

EFFECT OF COMBUSTOR-INLET CONDITIONS ON PERFORMANCE OF AN ANNULAR TURBOJET COMBUSTOR

By J. HOWARD CHILDS, RICHARD J. McCafferty, and OAKLEY W. SURINE

SUMMARY

The combustion performance and particularly the phenomenon of altitude operational limits was studied by operating the annular combustor of a turbojet engine over a range of conditions of air flow, inlet pressure, inlet temperature, and fuel flow. The combustor investigated was not the latest version of this combustor and the data are presented primarily because they are indicative of general trends and phenomena that apply to a large class of turbojet combustors.

Information was obtained on the combustion efficiencies, the effect on combustion of inlet variables, the altitude operational limits with two different fuels, the pressure losses in the combustor, the temperature and velocity profiles at the combustor outlet, the extent of afterburning, the fuel-injection characteristics, and the condition of the combustor basket.

The combustor operated at efficiencies above 90 percent and could produce a temperature rise far in excess of the engine requirement when the simulated altitude was 8000 feet or more below the operational limits. As the simulated altitude was progressively increased, the combustion efficiency and the obtainable temperature rise both decreased. Above the operational limits, the maximum obtainable temperature rise was below the value required for engine operation.

Investigations in which the combustor-inlet conditions of pressure, temperature, and velocity were independently altered through a wide range showed that as (1) the inlet pressure was decreased, (2) the inlet temperature was decreased, or (3) the inlet velocity was increased, the resulting unfavorable changes in combustor performance were as follows: (1) Resonant combustion appeared and became increasingly severe; (2) the combustion efficiency decreased; and (3) a maximum temperature rise began to appear in the curve of combustor temperature rise against fuel-air ratio. Both the maximum obtainable temperature rise and the fuel-air ratio at which it occurred decreased as the combustor-inlet conditions became more adverse. The effect of altitude previously noted and the existence of altitude operational limits are explained in terms of the effects of combustor-inlet conditions on performance.

INTRODUCTION

Investigations of turbojet-engine performance in the NACA Cleveland altitude wind tunnel have indicated that for each engine rotational speed an altitude exists above which engine operation is impossible. The performance of an annular combustor of a turbojet engine was therefore investigated at the NACA Cleveland laboratory to determine whether a correlation exists between the performance of the combustor and the altitude operational limits of the engine revealed by altitude-wind-tunnel research. The combustor investigated was not the latest model of this engine and the data are presented primarily as being indicative of general trends and phenomena applying to a large class of turbojet combustors.

Combustor operation was attempted under conditions simulating engine operation at various altitudes and engine speeds to determine the altitude operational limits imposed on the engine by the combustor. The altitude operational limit as imposed by the combustor was compared with the altitude operational limit of the engine in the altitude-wind-tunnel investigation. The inlet conditions to which the combustor was sensitive were also determined. The effect on combustor performance of independently varying each of the parameters—inlet static pressure, inlet temperature, inlet velocity, and fuel-air ratio—was studied. In order to augment these data and to illustrate how combustor performance limits altitude operation, an investigation was made of combustor performance under conditions simulating engine operation at several different rotational speeds at a constant altitude of 20,000 feet. Information on the total-pressure drop across the combustor, the temperature and velocity profiles at the combustor outlet, the extent of afterburning, the fuel-injection characteristics, and the condition of the combustor basket is also presented.

APPARATUS AND INSTRUMENTATION

COMBUSTOR

A sketch of the combustor is shown in figure 1. The combustor fills the annular space around the compressor-turbine shaft of a turbojet engine. The over-all length of the combustor is $23\frac{1}{4}$ inches. Air is admitted into the combustion zone by means of an annular basket perforated with longitudinal rows of holes ranging in size from $\frac{1}{2}$ -inch diameter at the upstream end to $\frac{1}{8}$ -inch at the downstream end. The fuel-injection system for the combustor consists of 24 nozzles (nominal capacity, 10.5 gal/hr; 80° hollow-cone spray; rated at 100 lb/sq in. pressure differential) equally spaced in the downstream side of a circular manifold on a $15\frac{1}{4}$ -inch pitch diameter. The fuel inlet is at the bottom of the manifold.

SETUP

The general arrangement of the setup is diagrammatically shown in figure 2. The combustor was connected to the laboratory air supplies and exhaust systems; the air quantities and the pressures to the combustor were regulated by remote-controlled valves.

For inlet-temperature regulation, a part of the air was burned with fuel in a preheater and then uniformly mixed with the rest of the air upstream of the combustor. A close check was maintained on the completeness of combustion in the preheater to insure that no appreciable combustibles contaminated the air. Use of such a preheater to produce a temperature rise of 200° F in the inlet air resulted in a consumption of 3.9 percent of the oxygen, increased the carbon dioxide content of the inlet air by 0.80 percent of the total air weight, and increased the moisture content by 0.36 percent of the total air weight.

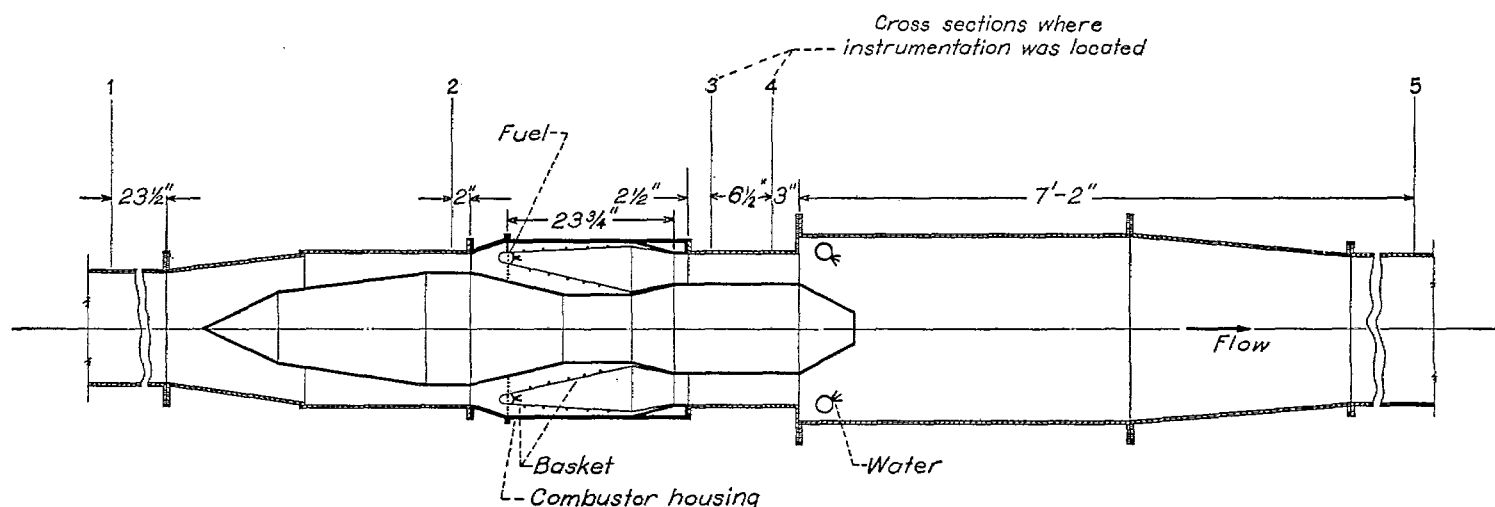


FIGURE 1.—Diagrammatic sketch of combustor showing inlet and outlet ducts and locations of instruments.

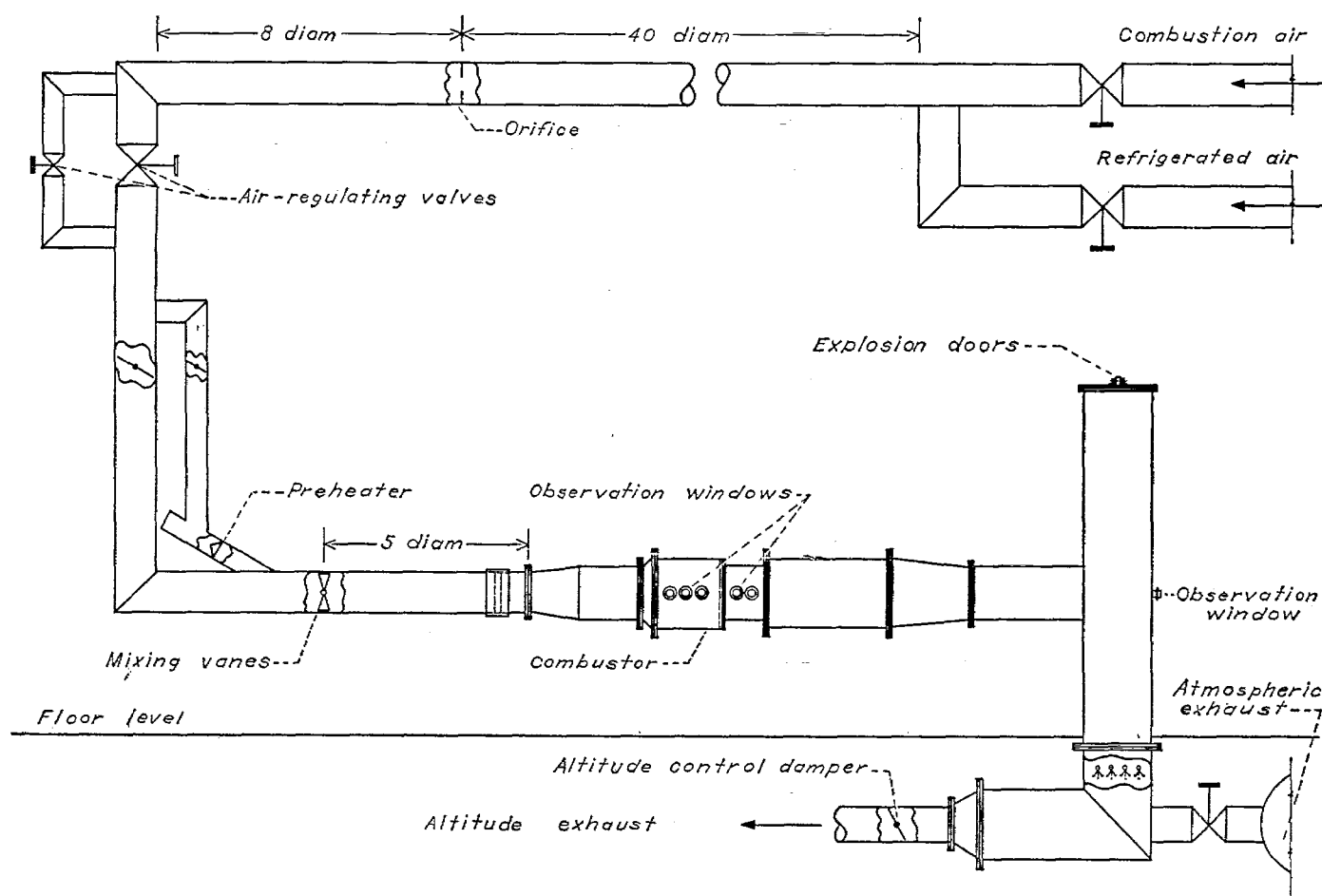


FIGURE 2.—Diagrammatic sketch of arrangement of combustor setup.

Observation windows for viewing the combustion were provided in the combustor housing and in the outlet duct immediately downstream of the combustor, as shown in figures 2 and 3. (The photograph of fig. 3 shows the side of the apparatus opposite to that of fig. 2.) Another observation window located in the downstream standpipe (fig. 2) provided an end view of the inside of the combustor.

The inlet and outlet ducts were fabricated according to the dimensions and the contours of the engine ducts leading to and from the combustor. Water sprays were installed in the pipe immediately downstream of the combustor-outlet

duct for use when the heat radiated from the downstream duct became excessive.

Mixing vanes followed by flow straighteners were installed in the inlet duct to give uniform temperature and velocity profiles at the combustor inlet. Maximum differences between individual readings of inlet temperature and mean temperature were about 5° F and occurred only on test runs with high preheat temperatures. The maximum and minimum local velocities deviated from the mean velocity about 5 percent for most runs. The fuel nozzles in the combustor were periodically calibrated and replaced when

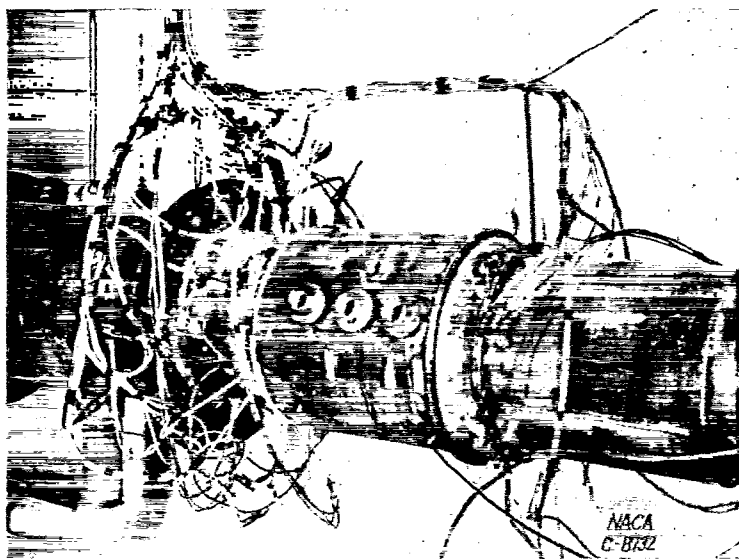


FIGURE 3.—Side view of combustor assembly.

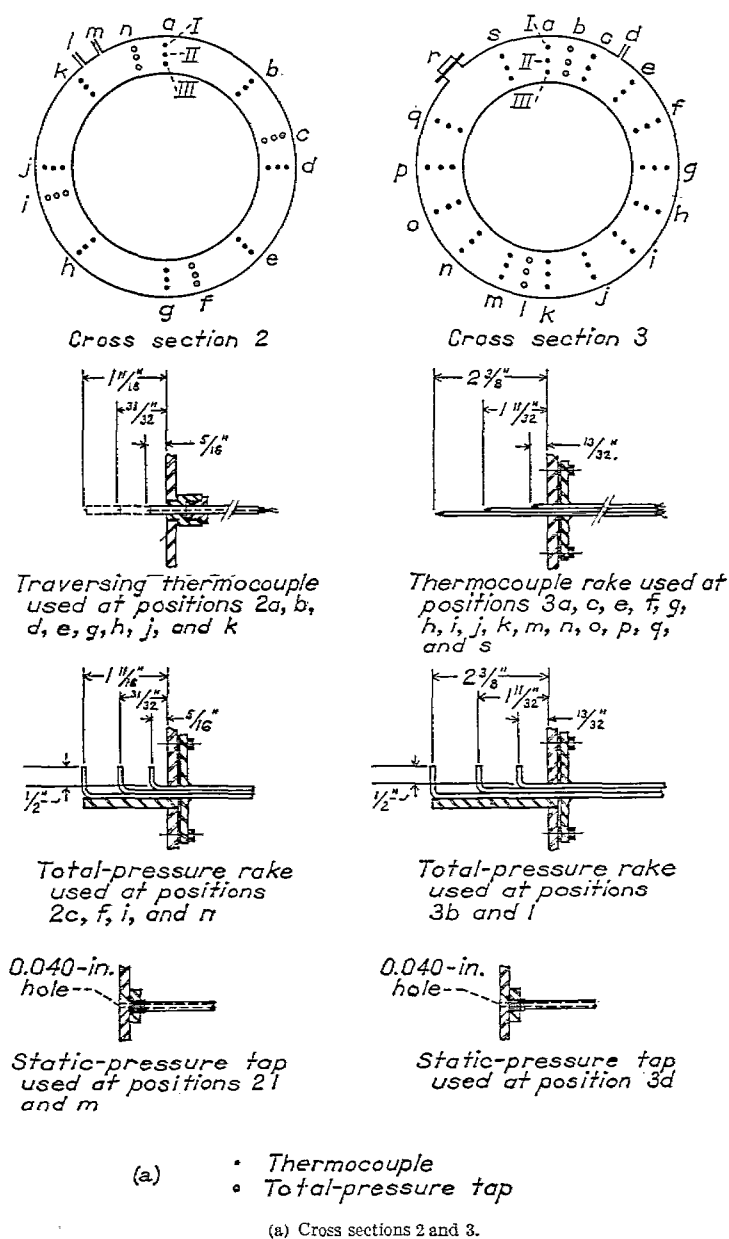


FIGURE 4.—Details of temperature- and pressure-measuring instruments and positions in various cross sections of inlet and outlet ducts. (Cross sections shown in fig. 1.)

necessary. For most runs these nozzles were well matched, having deviations of ± 3 percent from the mean fuel delivery when individually tested at a pressure differential of 25 pounds per square inch.

INSTRUMENTATION

The longitudinal section of the combustor and the adjacent ducting with a notation of the locations of instrumentation planes are shown in figure 1. Instrumentation plane 2 is located at the combustor inlet, which has a cross-sectional area of 0.647 square foot; instrumentation plane 3 is at the combustor outlet, where the annular cross-sectional area is 0.858 square foot.

Positions of thermocouple junctions and pressure taps in the various cross sections of the inlet and outlet ducts where measurements were made are shown in figure 4. In each cross section the instruments were located at centers of equal areas. At cross section 3 (fig. 4 (a)), 15 circumferential locations of thermocouple rakes are shown as they were initially arranged. Later in the investigation, the observation window at position r was replaced by an additional thermocouple rake. The positions at all cross sections were arranged clockwise as seen looking upstream.

Whenever there was no water spray immediately downstream of the combustor, the average exhaust-gas temperature at cross section 5 (fig. 4 (b)) was obtained by the use of a traversing shielded chromel-alumel thermocouple. Both horizontal and vertical traverses were made with this instrument until the temperature pattern at this cross section was established. The variation in temperature was not more than 50°F ; therefore, in later runs the instru-

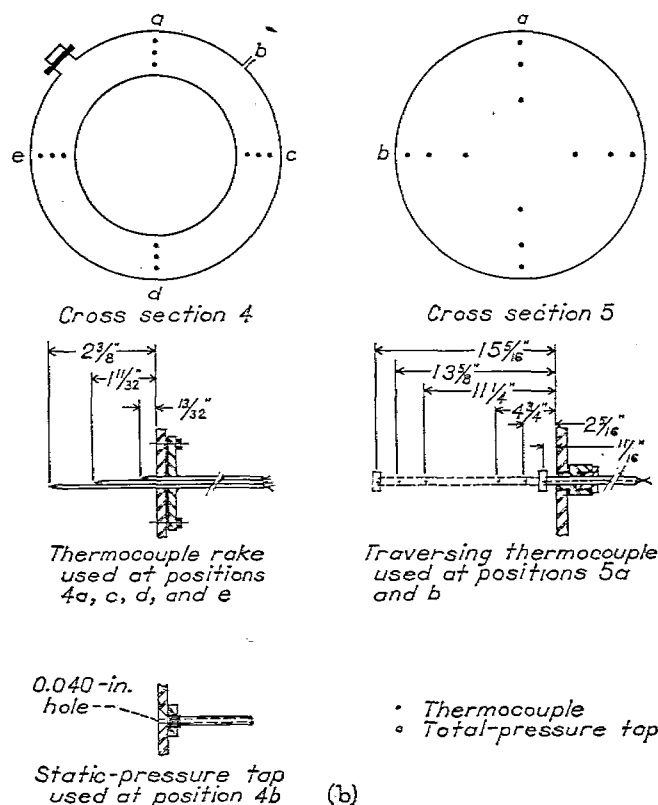


FIGURE 4.—Concluded.

ment was fixed in a stationary position where the temperature was approximately equal to the average temperature at cross section 5.

Thermocouple-equipped fuel nozzles were used in some runs. Iron-constantan thermocouples were so peened into the wall of the dome of each of three fuel nozzles that the metal temperatures could be determined. Each thermocouple junction was located halfway between the orifice and the hexagonal shoulder of the nozzle. The three nozzles were installed in the following positions in the manifold (looking upstream, reading counterclockwise with 0° at top of combustor): 22.5°, 97.5°, and 187.5°.

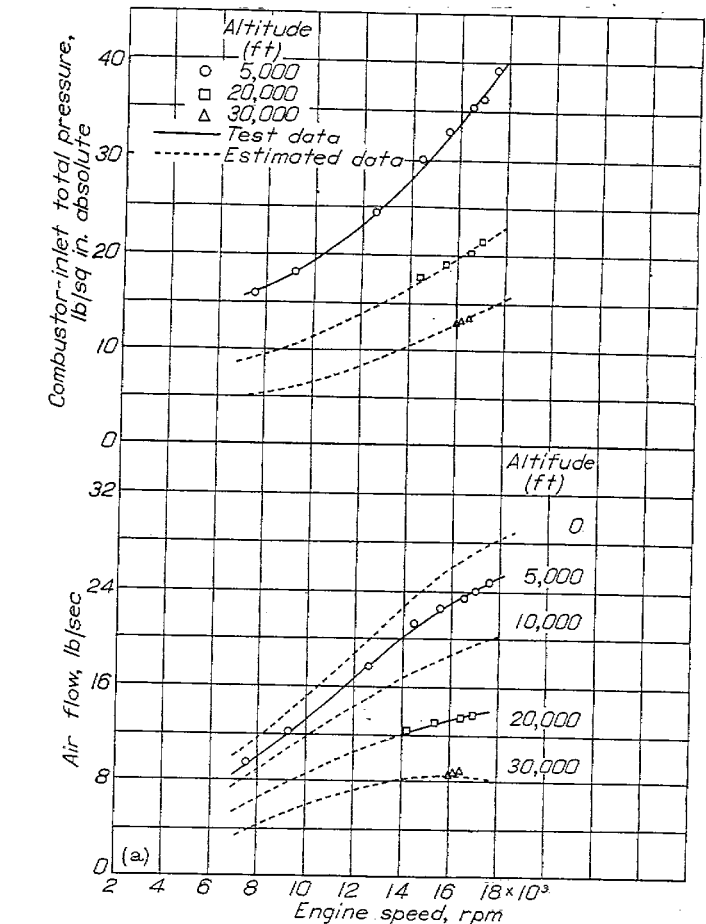
Thermocouples were connected through multiple switches to two calibrated self-balancing potentiometers, one with a range of -100° to 700° F for reading the inlet temperatures and one with a range of 400° to 2400° F for reading the outlet temperatures. The fuel flows to the combustor and the preheater were separately metered with calibrated rotameters. The pressure differential across the fuel nozzles was measured, when possible, by a 50-inch mercury manometer; higher differentials were determined by obtaining the fuel-manifold pressure with a Bourdon gage and correcting for the combustor-inlet pressure. The air flow was metered by a square-edged orifice installed according to A.S.M.E. specifications and located upstream of all regulating valves. Manometers were used to obtain pressure readings.

PROCEDURE

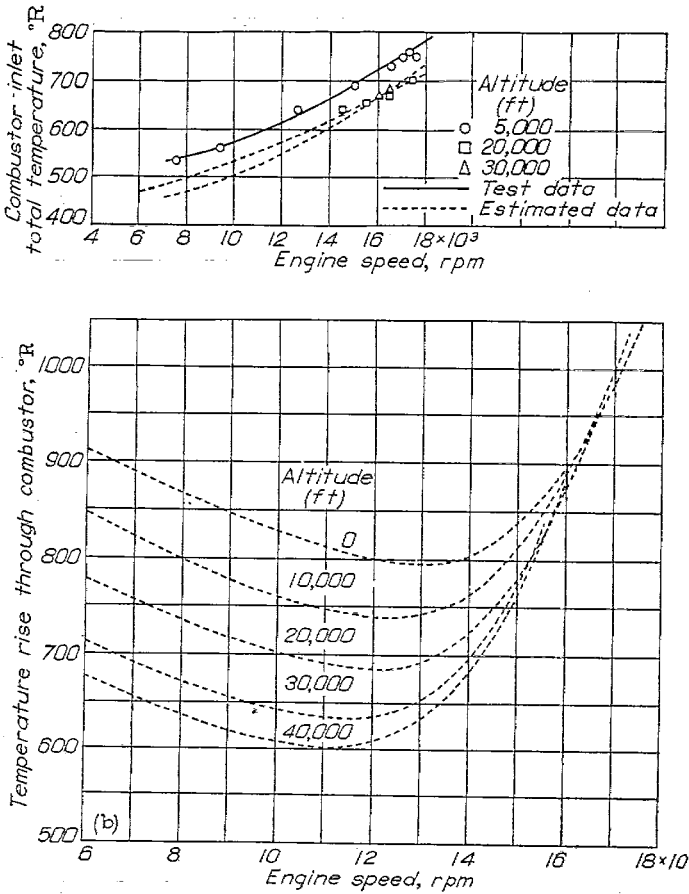
ALTITUDE OPERATIONAL LIMITS

In order to determine the altitude operational limits of the engine as imposed by the combustor, the performance was investigated with combustor-inlet conditions simulating engine operation over the range of altitudes and engine speeds where unsatisfactory combustion had been encountered in an altitude-wind-tunnel investigation of the complete engine. For each test point (corresponding to a simulated altitude and engine speed), the combustor operating conditions were taken from estimated performance curves of the engine for static (zero-ram) operation with the tail cone retracted. Any complete set of data can be satisfactorily used as a standard for determining the effect of inlet conditions upon combustion and for revealing the important phenomena and trends. The data used (fig. 5) were supplied by the Bureau of Aeronautics, Navy Department, and were based on the latest engine tests and performance estimates.

The method of determining the altitude operational limits consisted in maintaining the combustor-inlet conditions at the predetermined values (fig. 5) for each altitude-engine-speed point and gradually varying the fuel flow through a wide range. All points at which the highest obtainable combustor-temperature rise was below that required for nonaccelerating operation of the engine (fig. 5 (b)) were considered within the nonoperational range of the engine;



(a) Combustor-inlet total pressure and air flow for various altitudes and engine speeds.



(b) Combustor-inlet total temperature and temperature rise through combustor for various altitudes and engine speeds.

FIGURE 5.—Engine conditions used in investigation of combustor. Static engine operation; tail cone retracted. (Data from Bureau of Aeronautics, Navy Department.)

all points at which the required temperature rise could be obtained were considered within the operational range. Data were recorded and combustion characteristics were noted as each of the following events occurred: (1) A mean combustor-outlet temperature was reached that was equal to or slightly above the temperature required for non-accelerating engine operation; (2) the type of combustion changed radically; (3) a peak in the mean combustor-outlet temperature was reached; (4) some localized outlet temperatures exceeded the potentiometer range (2400°F) and were considered unsafe for the instruments, and therefore further increase in fuel flow was inadvisable; and (5) the combustion ceased (a rich-limit blow-out). The sequence and the number of these events varied for the different test points.

The runs were first made with AN-F-22 fuel and then repeated with AN-F-28, Amendment-3, fuel. The important constants for the two fuels appear in the following table:

Fuel	Lower heating value (Btu/lb)	Hydrogen-carbon ratio	Specific gravity $60^{\circ}/60^{\circ}\text{F}$	A.S.T.M. boiling points ($^{\circ}\text{F}$)			Tetraethyl lead (ml/gal)
				Initial	50-percent	Final	
AN-F-22	19,000	0.182	0.699	113	170	233	0
AN-F-28, Amendment-3	18,600	.174	.725	103	213	328	4.55

EFFECT OF COMBUSTOR-INLET CONDITIONS ON PERFORMANCE

For the investigation of the effect of combustor-inlet conditions on performance, AN-F-22 fuel was used. For the initial part of this study, a point was selected in the range of operation where unsatisfactory combustion occurred that corresponded to an engine speed of 10,000 rpm and an altitude of 16,600 feet. The combustor-inlet pressure, temperature, and velocity were maintained at values simulating engine operation at this altitude-engine-speed point; the fuel flow was altered; and data were taken at each of several fuel-air ratios. One of the three combustor-inlet parameters (pressure, temperature, or velocity) was then maintained at some new value, the other two parameters were maintained at the original values, and the fuel flow was again altered. This procedure was continued until each of the combustor-inlet parameters had been varied independently of the others. Combustor-inlet velocity rather than air mass flow was chosen as a parameter because the available combustion time is more directly related to flow velocity than to mass flow.

For the second part of this study, a point corresponding to an engine speed of 15,500 rpm and an altitude of 24,000 feet was selected in order to determine the effect of combustor-inlet conditions in this altitude-engine-speed range. Each of the combustor-inlet parameters was independently altered from the value simulating engine operation at this point.

COMBUSTOR PERFORMANCE AT SEVERAL SIMULATED ENGINE SPEEDS AT CONSTANT ALTITUDE

In order to illustrate how faulty combustor performance sets the altitude operational limits, the combustor was operated with inlet conditions simulating engine operation at seven different rotational speeds at an altitude of 20,000 feet. For each simulated altitude-engine-speed condition, the flow of AN-F-22 fuel was increased until no higher mean

combustor-outlet temperature could be obtained, blow-out occurred, or local outlet temperatures became excessive and endangered the instrumentation. Data were taken at several fuel-air ratios for each set of combustor-inlet conditions.

METHODS OF CALCULATION

The average velocities and velocity pressures at cross sections 2 and 3 were computed from the air flow, the fuel flow, and the average temperatures and static pressures measured at these cross sections. The total-pressure drop through the combustor was obtained as follows: Static pressures at the combustor inlet and the combustor outlet were measured; the velocity pressures based on the average velocities were added to these static pressures to give total pressures at the combustor inlet and the combustor outlet; and the difference between these values was taken as the drop in total pressure through the combustor.

In order to determine velocity profiles, the local velocities at several points were computed from the measured values of temperature and total pressure at those points together with the static pressure at that cross section.

Thermocouple indications were taken as true values of temperature without correction for radiation or stagnation effects.

RESULTS AND DISCUSSION

ALTITUDE OPERATIONAL LIMITS

The data obtained in the investigation to determine the altitude operational limits are summarized in tables I and II. Whenever several individual readings of combustor-outlet temperature fell below the potentiometer range (400°F), the mean combustor-outlet temperatures and dependent calculated data were omitted from the tables. Determination of individual readings below 400°F was considered unnecessary because the mean outlet temperatures that resulted with such low readings were in all cases far below the requirement of the engine for nonaccelerating operation. The points labeled "no combustion" (points 4 and 6, table I) are those where repeated attempts produced no burning at any fuel flow.

Altitude operational limits of the jet-propulsion engine, as determined by tests of the combustor using AN-F-22 and AN-F-28, Amendment-3, fuels are presented in figures 6 (a) and 6 (b), respectively. The curves separate the region where the combustor-outlet temperatures attainable were sufficient from the region where the combustor-outlet temperatures attainable were insufficient for nonaccelerating operation of the engines. For convenience in referring to tables I and II, the data points on the figures are identified by numbers. The minimum operational ceiling with AN-F-22 fuel (fig. 6 (a)) was at an altitude of 16,400 feet and occurred at a simulated engine speed of 8000 rpm; at a simulated engine speed of 17,500 rpm the operation was satisfactory to an altitude of 34,000 feet. With AN-F-28, Amendment-3, fuel (fig. 6 (b)), the minimum ceiling was at 14,600 feet and also occurred at a simulated engine speed of 8000 rpm; at engine speeds above 17,000 rpm, operation was satisfactory to altitudes higher than 30,000 feet.

Variations other than those indicated by the operational-limit curves were observed in the combustion characteristics of the two fuels. Ignition was easier with AN-F-22 fuel

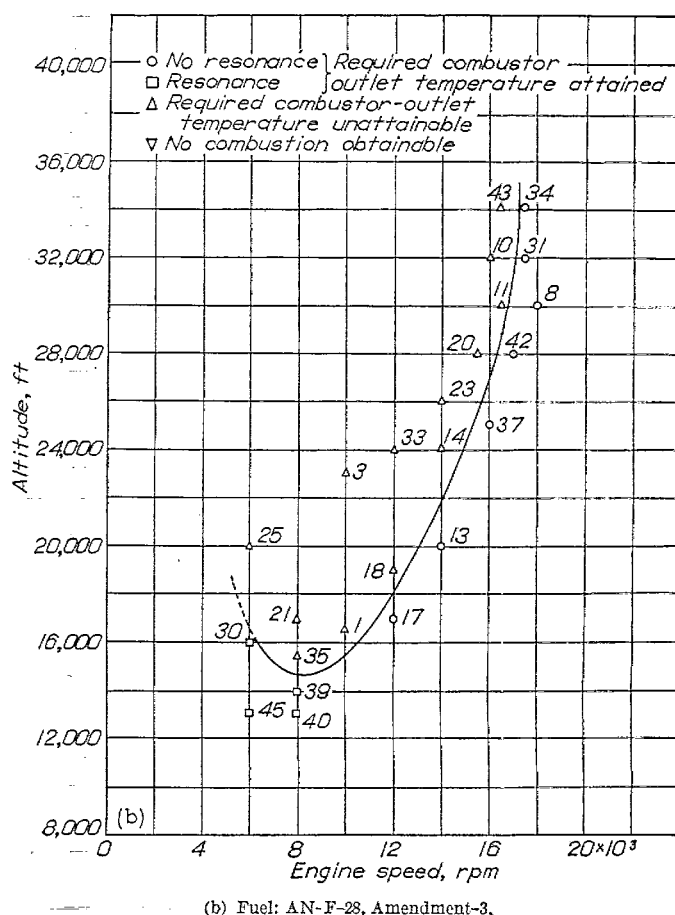
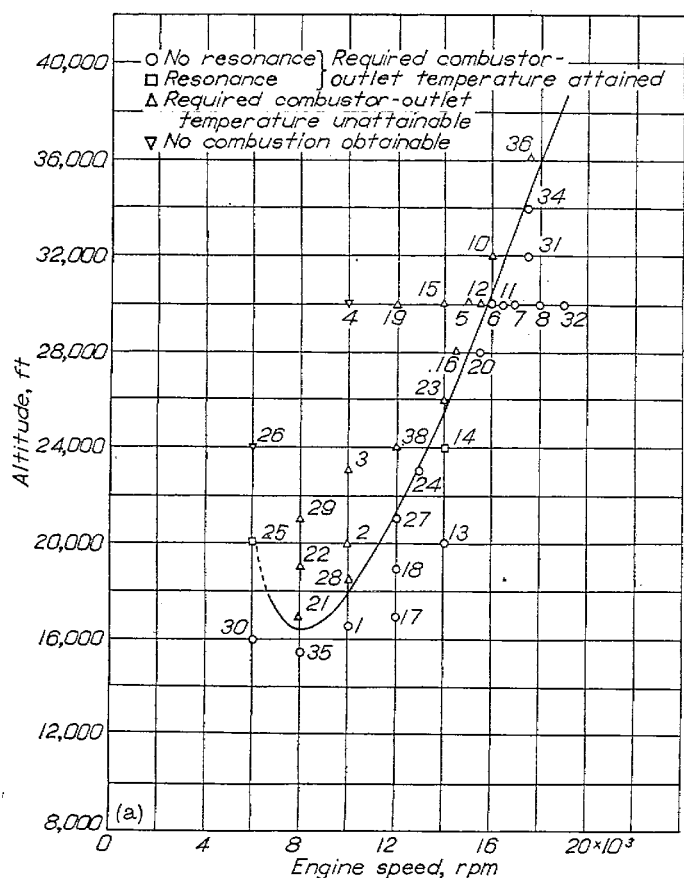


FIGURE 6.—Altitude operational limits of combustor under conditions simulating static operation of engine with tail cone retracted. (Point numbers listed in table I.)

than with AN-F-28 fuel. In the region immediately below the altitude-operational-limit curves, AN-F-28 fuel generally produced more flickering of the flames than did AN-F-22 fuel. When AN-F-28 fuel was used at simulated engine speeds below 12,000 rpm, the flame flickered and fluctuations occurred in the combustor-outlet temperatures at altitudes as much as 3000 feet below the operational-limit curve (fig. 6 (b)). When operating with either fuel at simulated engine speeds below 8000 rpm, combustion sometimes ceased when the fuel flow was decreased to low values (lean-limit blow-out). This phenomenon was not encountered at high simulated engine speeds.

The combustor operated at efficiencies above 90 percent and was capable of producing outlet temperatures far in excess of the engine requirement when the simulated altitude was 8000 feet or more below the operational limits. As the simulated altitude was increased: (1) Resonant combustion appeared and became increasingly severe; (2) combustion efficiency decreased; and (3) temperature rise through the combustor began to pass through a maximum value (with variation of fuel-air ratio) within the fuel-air-ratio range investigated. Both the maximum temperature rise obtainable and the fuel-air ratio at which it occurred decreased as the simulated altitude was increased. The resonant combustion, which was encountered at altitudes near the operational limits, was characterized by one or more of the following conditions: rapid flickering at the base of the flame, noisy vibration of the combustor and adjacent ducting, and fluctuation of the combustor-outlet temperatures. (In order to distinguish between the several types of resonance, the

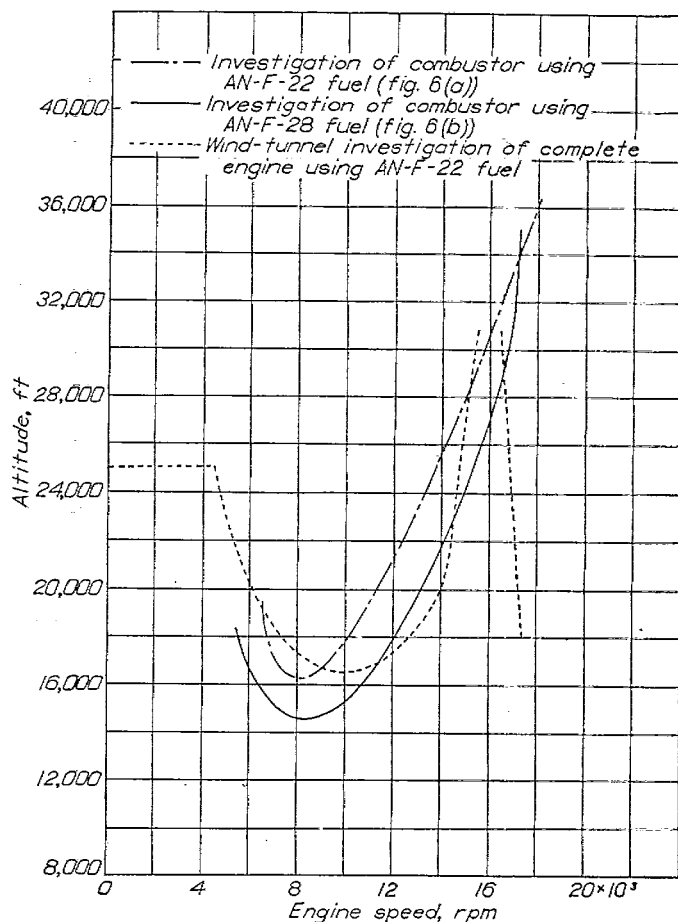


FIGURE 7.—Comparison of altitude operational limits of jet-propulsion engine as determined by wind-tunnel investigation of complete engine using AN-F-22 fuel and by investigations on combustor operating with AN-F-22 and AN-F-28 fuels.

kind of combustion occurring during each run was given a letter designation.)

The altitude-operational-limit curves of figure 6 compared with the corresponding curve determined by altitude-wind-tunnel tests of the complete engine using AN-F-22 fuel are shown in figure 7. Operational failures at high engine speeds (above 16,000 rpm), which were encountered in the wind-tunnel investigation of the engine, did not occur in the combustor tests. One possible cause of this difference might be that nonuniform flow conditions existed at the combustor inlet in the engine, whereas in the combustor studies a uniform inlet-velocity profile was maintained.

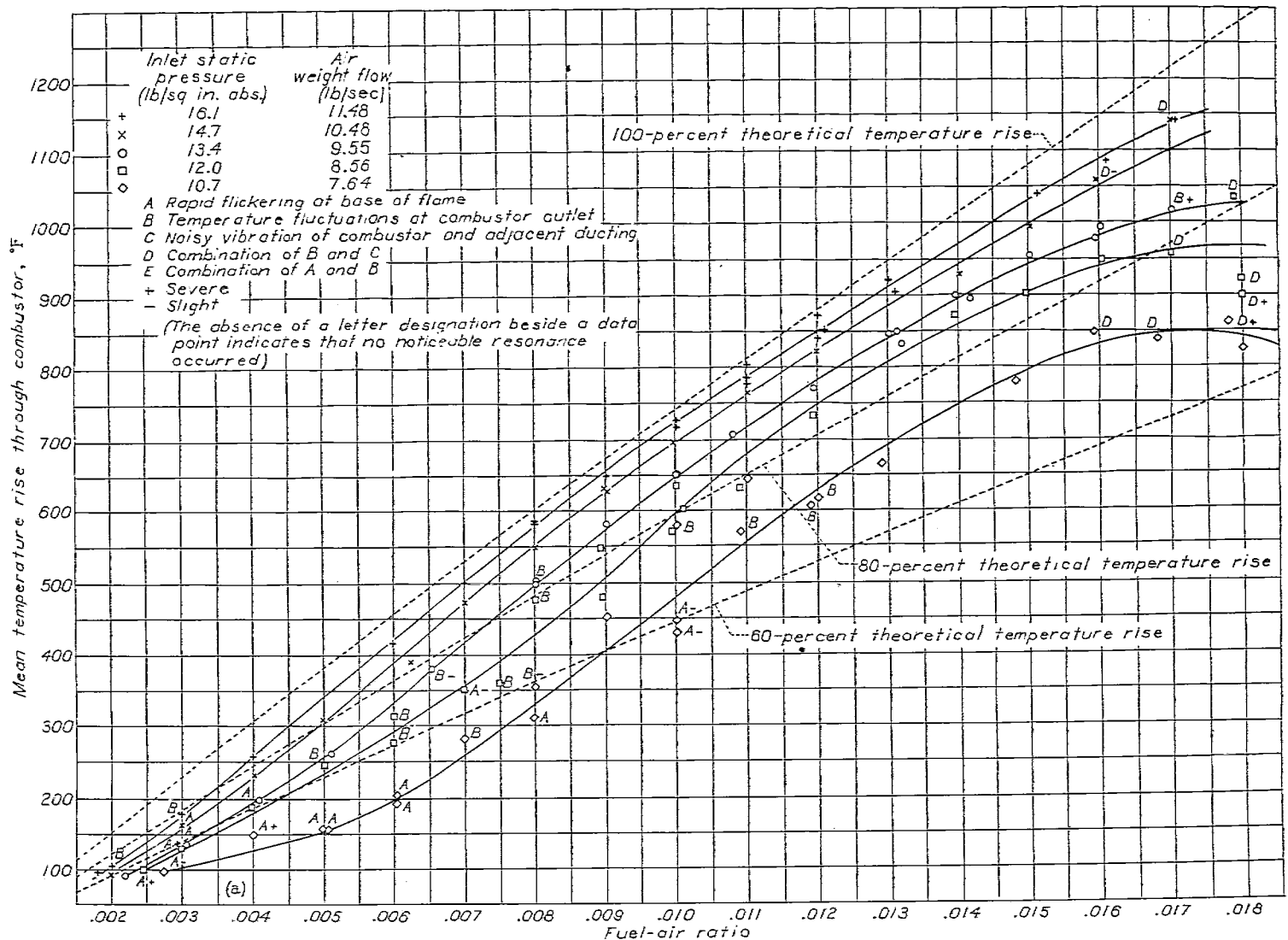
EFFECT OF COMBUSTOR-INLET CONDITIONS ON PERFORMANCE

The effect of combustor-inlet conditions on the performance of the combustor is shown in figures 8 and 9, where the mean of the measured temperature rise through the combustor is plotted as a function of fuel-air ratio. For estimation of combustion efficiencies, curves for 60 percent, 80 percent, and 100 percent of the theoretical temperature rise are included in both figures. The theoretical-temperature-rise curves of figure 8 are based on an inlet temperature

of 65° F; the corresponding curves of figure 9 are based on an inlet temperature of 190° F.

The curves in figure 8 show the effects on combustion of independently varying the combustor-inlet pressure, temperature, and velocity from conditions that simulate zero-ram engine operation at an engine speed of 10,000 rpm and an altitude of 16,600 feet.

The effect on combustor performance of altering the combustor-inlet static pressure while maintaining the inlet temperature and velocity constant is shown in figure 8 (a). When the inlet pressure was high, the combustion efficiency was above 95 percent and the temperature rise through the combustor increased throughout the range of fuel-air ratios investigated. Operation at fuel-air ratios higher than 0.018 was not attempted because local outlet temperatures exceeded the safe limits of the instrumentation. When the inlet pressure was low, the combustion efficiency was low and the temperature rise through the combustor passed through a maximum value at a fuel-air ratio much leaner than the over-all stoichiometric mixture; beyond this value the combustion efficiency decreased rapidly with increase in the fuel-air ratio. Both the maximum temperature rise at-



(a) Effect of altering static pressure at combustor inlet. Inlet temperature, 65° F; inlet velocity, 214 feet per second.

FIGURE 8.—Variation of mean temperature rise through combustor with fuel-air ratio for combustor-inlet conditions independently altered from values simulating engine operation at rotational speed of 10,000 rpm and altitude of 16,600 feet.

tainable and the fuel-air ratio at which it occurred decreased as the inlet pressure was decreased. Resonance always became severe as the fuel-air ratio was increased past the value giving the maximum attainable temperature rise and a rich-limit blow-out occurred. Changes in the slopes of the combustor performance curves were always accompanied by changes in the type of operation, as shown by letter designations indicating various types of resonance beside the data points on the figure.

Similar data showing the effect of altering the combustor-inlet temperature are presented in figure 8 (b). Comparison of figures 8 (a) and 8 (b) indicates that a decrease in combustor-inlet temperature produced the same general effects on performance as a decrease in combustor-inlet pressure.

Figure 8 (c) shows the effect of altering the combustor-inlet velocity. An increase in the air velocity had the same general effect on performance as a decrease in inlet pressure or in inlet temperature.

Similar results obtained with each of the combustor-inlet parameters independently varied from conditions simulating engine operation at 15,500 rpm and an altitude of 24,000 feet are presented in figure 9; each of the combustor-inlet parameters had the same general effect on performance at the high-altitude, high-engine-speed point as at the low-altitude, low-engine-speed point of figure 8.

In each of the families of curves shown in figures 8 and 9, the lower curves in the family fall farther apart although the curve parameters change in nearly equal increments, which

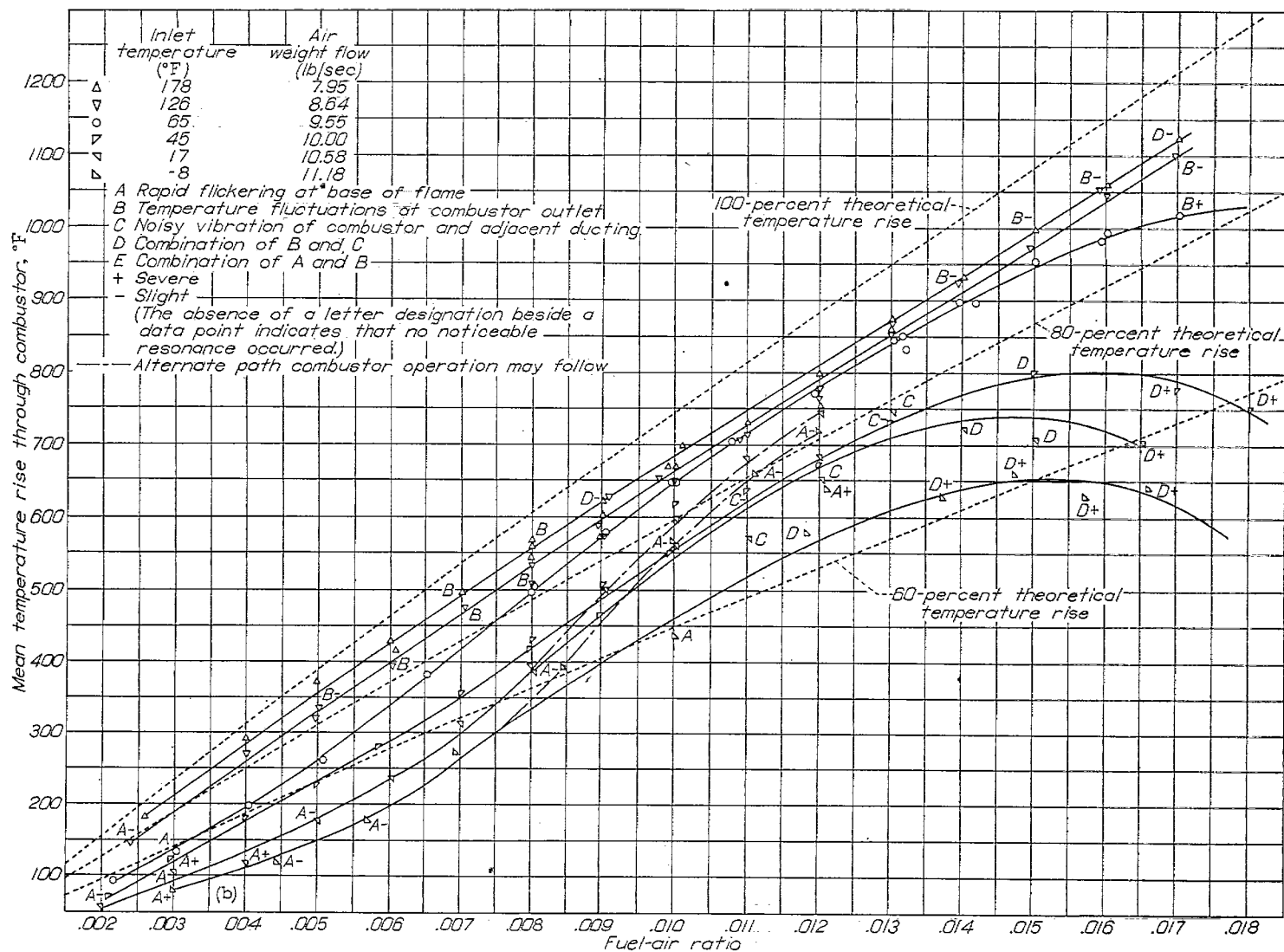


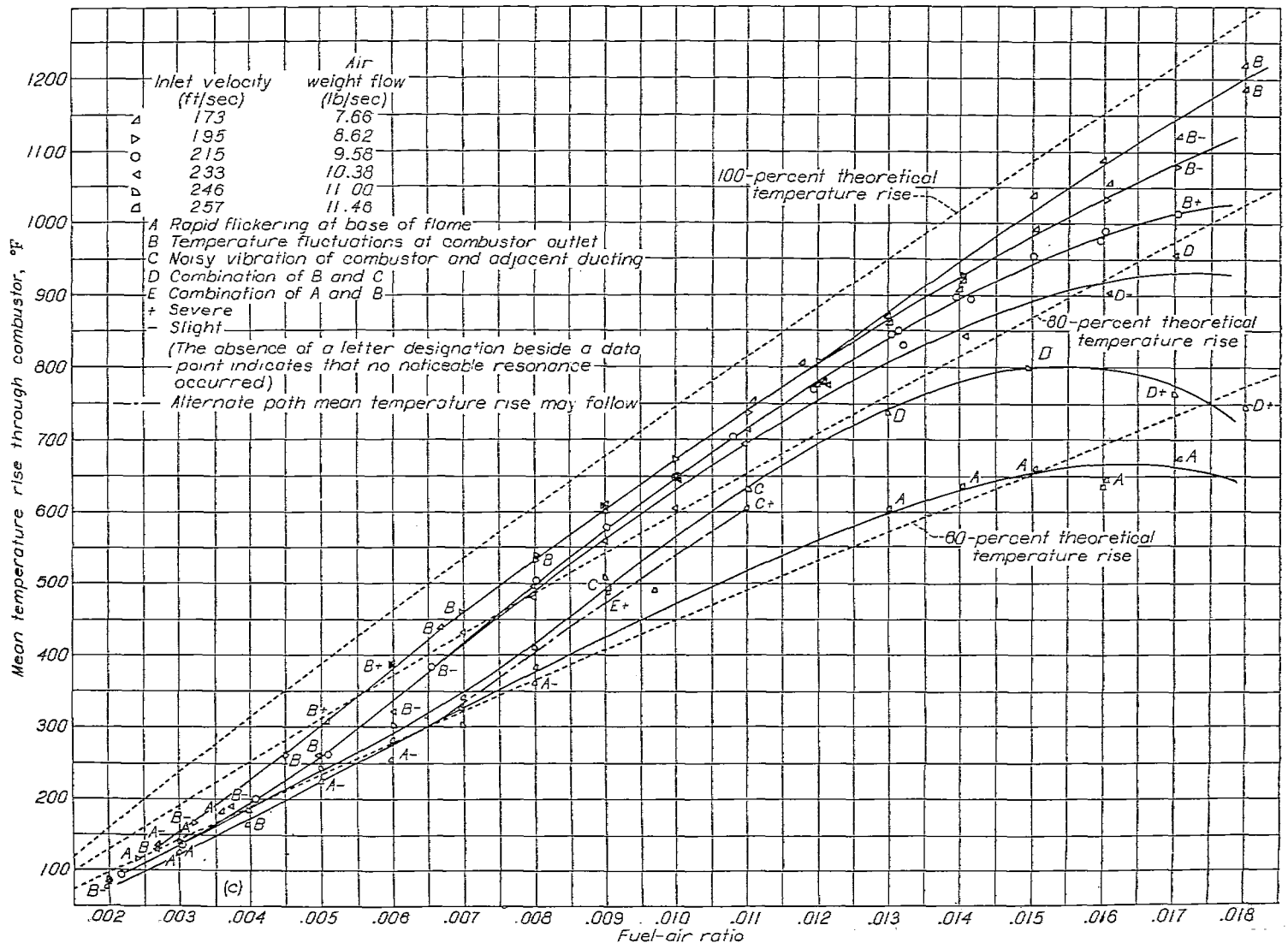
FIGURE 8.—Continued.

indicates that a given increment in any one of the combustor-inlet parameters produces more of an effect upon combustion performance as that parameter becomes more adverse to combustion.

Sharp breaks occur in some of the curves of figure 9. Such discontinuities were accompanied by equally sudden changes in the type of combustion. For example, at fuel-air ratios below 0.0141, where the break begins in the lowest curve in figure 9 (c), the combustor operated with very little resonance; at fuel-air ratios above 0.0145, the flame moved to a new seat about 2 inches downstream of the fuel nozzles and became intermittent and noisy. The fuel-air ratio at which such abrupt changes in operation occurred varied

slightly according to whether the point was approached by increasing or by decreasing the fuel flow and according to the rapidity with which the fuel flow was changed. Unless sudden changes in the type of combustion were observed, discontinuities were not drawn in the curves of figure 9.

In check runs it was found that the outlet temperature obtained for a given fuel-air ratio could be reproduced only when operating under conditions normally giving little resonance. When resonance was pronounced, as the fuel flow was increased (all other conditions held constant), the flame would sometimes be extinguished at fuel-air ratios below those where operation had continued in previous attempts. Some points where such rich-limit blow-outs occurred are



(c) Effect of altering velocity at combustor inlet. Inlet temperature, 68° F; inlet static pressure, 13.4 pounds per square inch absolute.

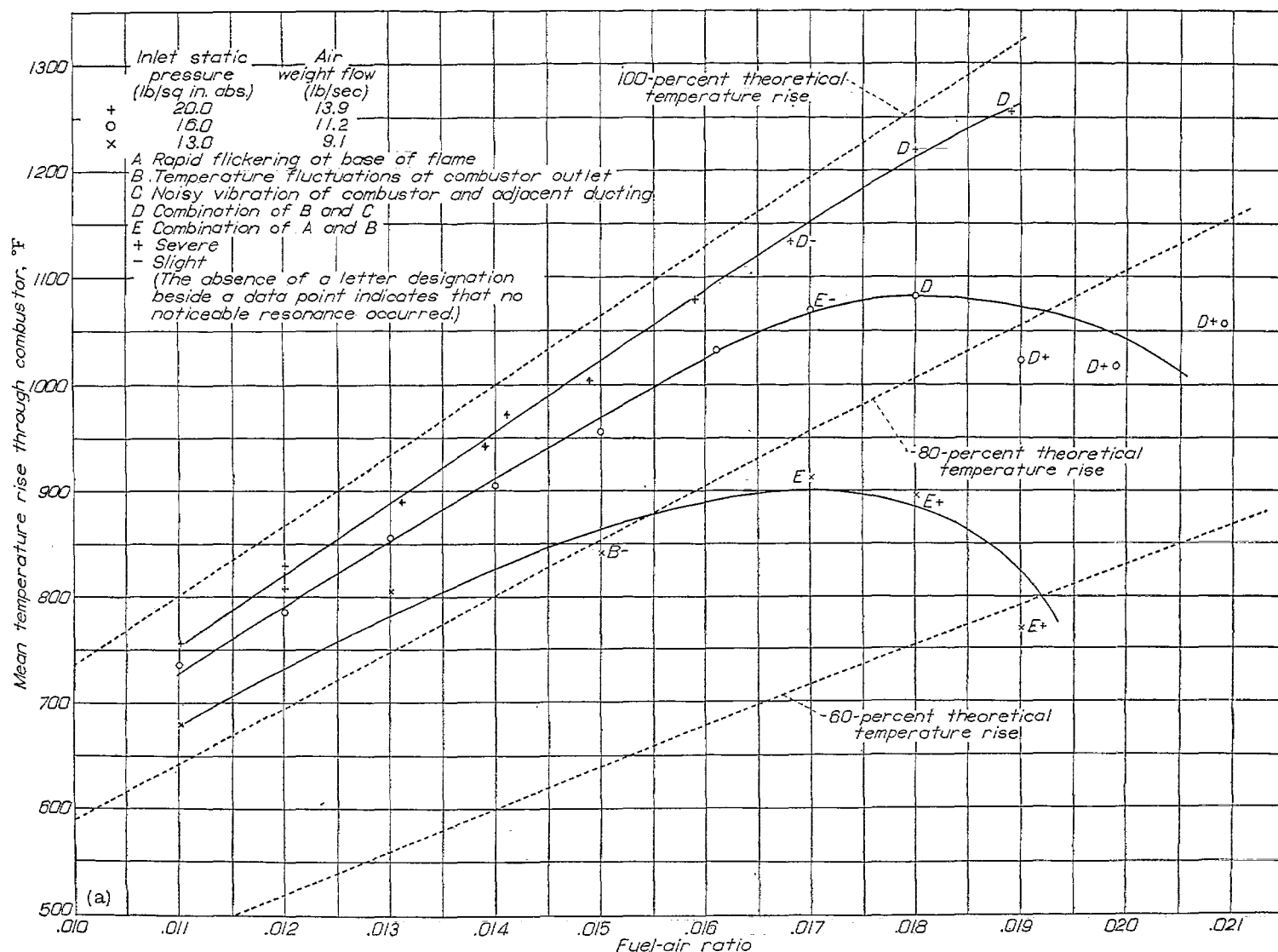
FIGURE 8.—Concluded.

indicated in figures 9 (b) and 9 (c). In the intermediate fuel-air-ratio range of figures 8 (b) and 8 (c), dual performance curves for the combustor were obtained and these curves are shown by dot-and-dash lines. This tendency of the combustor to drift into different modes of operation existed when operating under conditions that gave resonant combustion.

COMBUSTOR PERFORMANCE AT SEVERAL SIMULATED ENGINE SPEEDS AT CONSTANT ALTITUDE

In order to illustrate how faulty combustor performance imposes the altitude operational limits, figures 10 and 11 are presented. Results are shown in figure 10 for which data were taken over a range of fuel-air ratios with combustor-

inlet conditions simulating engine operation at each of seven engine speeds at an altitude of 20,000 feet. The mean of the measured values of temperature rise through the combustor are plotted against the fuel-air ratios used to obtain them. Each of the resulting curves has the same general shape as the curves of figures 8 and 9. Curves for 100-percent, 80-percent, and 60-percent theoretical temperature rise are indicated by dashed lines. The points where the curves surpass the temperature-rise requirement of the engine are indicated by symbols that are connected by a dotted line. At the intermediate simulated engine speeds (8000 and 10,000 rpm) blow-out occurred before the temperature rise reached the engine requirement.



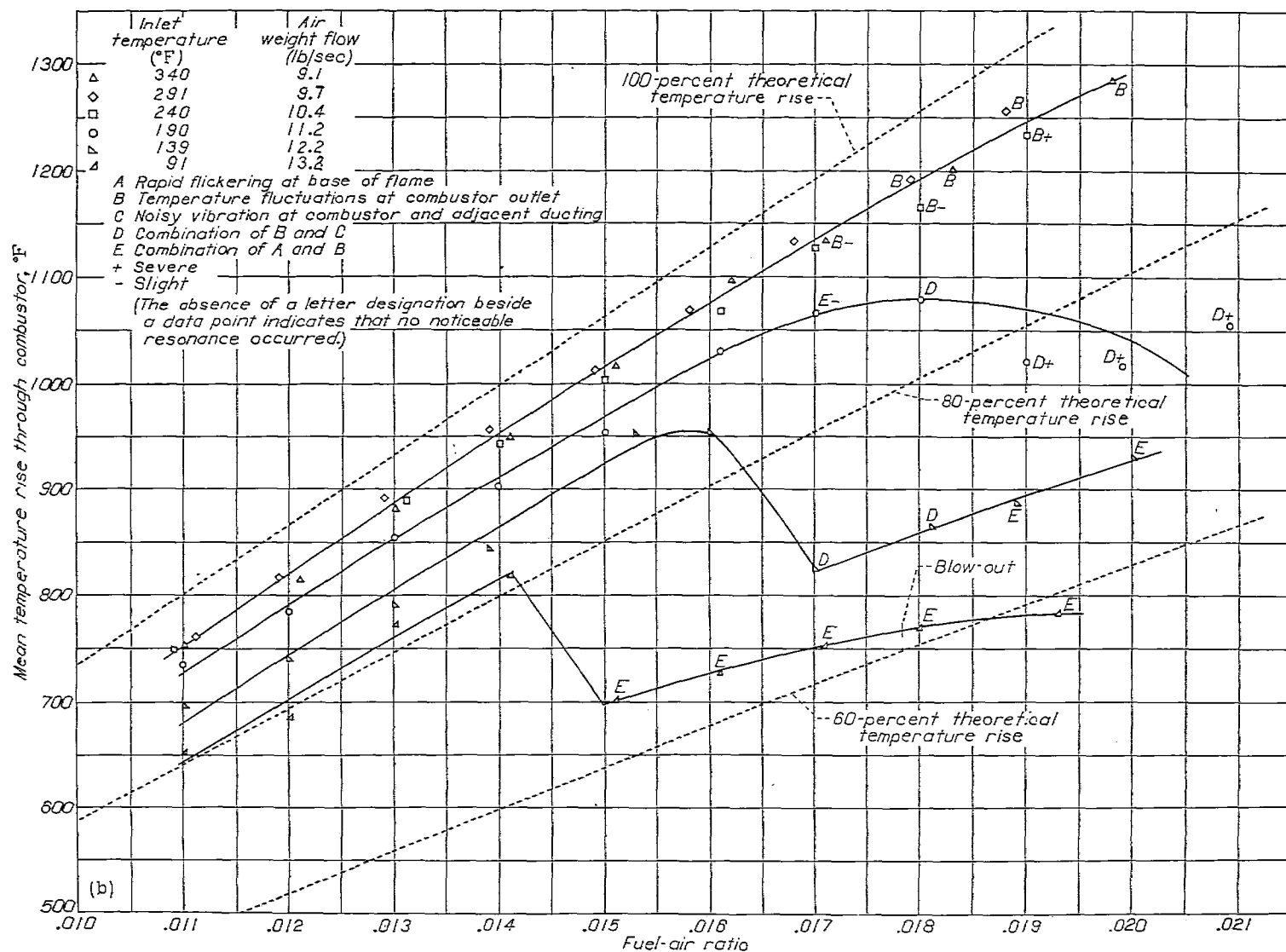
(a) Effect of altering static pressure at combustor inlet. Inlet temperature, 190° F; inlet velocity, 260 feet per second.

FIGURE 9.—Variation of mean temperature rise through combustor with fuel-air ratio for combustor-inlet conditions independently altered from values simulating engine operation at rotational speed of 15,500 rpm and altitude of 24,000 feet.

The temperature-rise requirement of the engine for nonaccelerating operation at various engine speeds at an altitude of 20,000 feet is shown in figure 11. Values of the maximum temperature rise obtainable with various simulated engine speeds at this altitude (taken from the peaks of the curves in fig. 10) are connected by a dotted line. The resulting curve falls below the temperature-rise-requirement curve between engine speeds of 6500 and 11,300 rpm. The nonoperational range therefore exists between 6500 and 11,300 rpm at an altitude of 20,000 feet.

An analysis of the causes of the altitude operational limits can be made by following a constant-altitude path at 20,000 feet, going from low to high engine speeds, observing what

happens to engine performance (figs. 10 and 11), and examining these happenings in terms of the effects of the combustor-inlet conditions on combustion performance. The combustor-inlet pressures, temperatures, and velocities existing in the engine at an altitude of 20,000 feet at various rotational speeds are shown in figure 11. Starting at an engine speed of 6000 rpm, the combustor produces the temperature-rise requirement of the engine. At this point, the combustor-inlet pressure and temperature are relatively low, and both are therefore adverse to combustion. The inlet velocity is very low, however, and a low velocity has a favorable effect on combustion enabling the combustor to give the required temperature rise.



(b) Effect of altering temperature at combustor inlet. Inlet static pressure, 16.0 pounds per square inch absolute; inlet velocity, 260 feet per second.

FIGURE 9.—Continued.

As the engine is accelerated to higher engine speeds, the combustor-inlet pressure and temperature increase; these changes are beneficial to combustion. At the same time, however, the inlet velocity increases very rapidly and this change has a detrimental effect on combustion. The unfavorable effect of the rapidly increasing inlet velocity more than counterbalances the beneficial changes in the other operating conditions, as is evidenced by the decrease in temperature rise obtainable, until the combustor ceases to meet the engine requirements when a speed of 6500 rpm is reached.

As the simulated engine speed is increased through the nonoperational region, the inlet pressure and temperature increase at accelerating rates whereas the inlet velocity increases at a decelerating rate with increase in simulated engine speed. At a simulated speed of about 10,000 rpm, the favorable effects of the rapidly increasing inlet pressure and temperature become large enough to offset the adverse effect of the increasing inlet velocity and the temperature rise obtainable begins to increase with simulated engine speed. At a speed of 11,300 rpm, the temperature rise obtainable is equal to the temperature rise required. Above

an engine speed of 11,300 rpm, the inlet velocity increases only slightly and approaches a maximum value whereas the inlet pressure and temperature increase rapidly and bring the combustor farther into the satisfactory operating range.

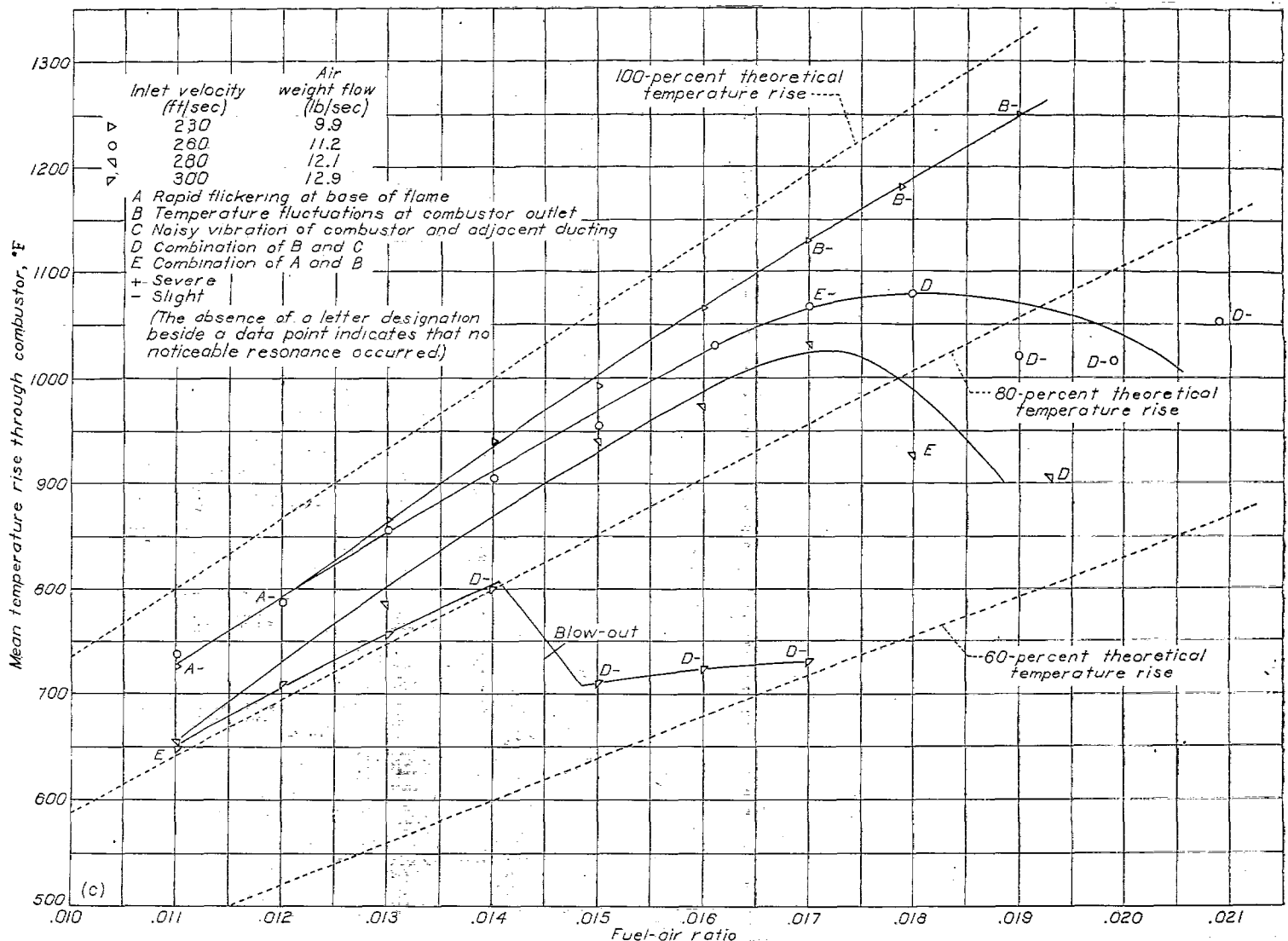
PRESSURE DROP THROUGH COMBUSTOR

A correlation of the combustor total-pressure drop is presented in figure 12. The ratio of the total-pressure drop to the inlet dynamic pressure $\Delta P_{2-3}/q_2$ is plotted against the ratio of the combustor-inlet density to the average combustor-outlet density ρ_2/ρ_3 . In the appendix, $\Delta P_{2-3}/q_2$ is shown to be a linear function of ρ_2/ρ_3 , and the predicted straight-line correlation is obtained in figure 12.

The derivation of the relation

$$\frac{\Delta P_{2-3}}{q_2} = f(\rho_2/\rho_3)$$

presented in the appendix assumes that at cross section 2 the inlet dynamic pressure q_2 is the effective value of q ; the relation is also valid, however, if the effective value of q has a fixed ratio to q_2 . In the annular combustor, both the cross-sectional areas of the flow passages and the ratio of air mass



(c) Effect of altering velocity at combustor inlet. Inlet temperature, 190° F; inlet static pressure, 16.0 pounds per square inch absolute.

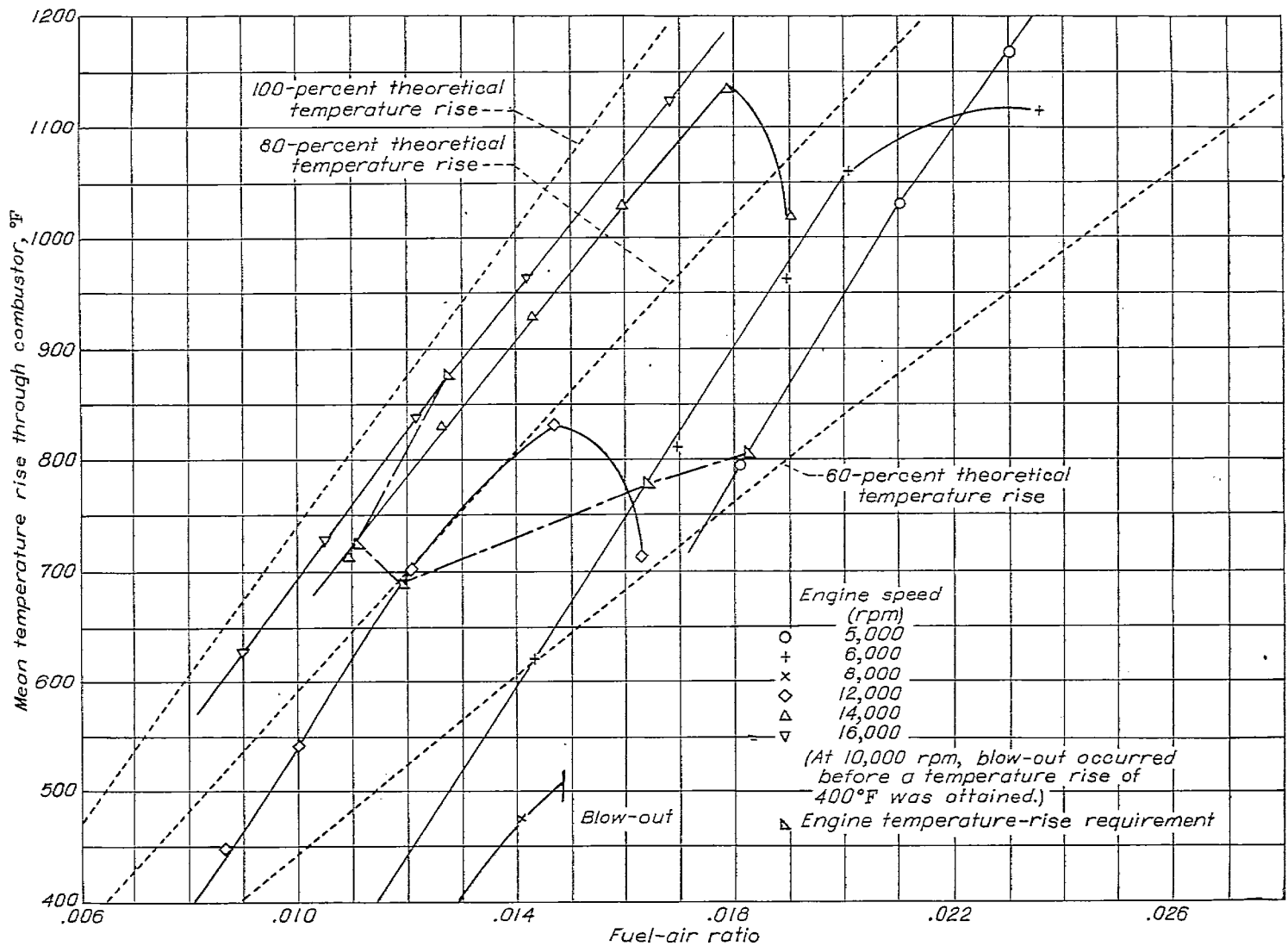


FIGURE 10.—Operation of combustor with inlet conditions corresponding to various engine speeds at altitude of 20,000 feet. Static operation; tail cone retracted.

in the combustion zone to the total air mass continually change when passing downstream through the combustor. The ratio of the effective q to q_2 therefore continually changes as the flame seat moves downstream. Inasmuch as the location of the flame seat changed, especially under operating conditions that promoted resonant combustion, the preceding relation cannot be expected to hold exactly for this combustor and some scatter of the data points, as indicated in figure 12, might be expected.

The isothermal $\Delta P_{2-3}/q_2$ is 1.62; and when ρ_2/ρ_3 is 2.8, $\Delta P_{2-3}/q_2$ is about 2.1.

TEMPERATURE AND VELOCITY PROFILES AT COMBUSTOR OUTLET

Combustor-outlet temperature profiles for four representative runs are shown in figure 13. The combustor-inlet conditions for the run presented in figure 13 (a) simulate engine operation at an engine speed of 10,000 rpm and an altitude of 16,600 feet and the mean combustor-outlet temperature is 150° F above required normal-operation temperature. The inlet conditions are approximately the same for the run presented in figure 13 (b) and the mean outlet temperature is about 220° F higher than required normal-operation temperature. In figure 13 (a) the mean outlet temperature is 968° F, the minimum recorded local temperature is 718° F, the maximum recorded local temperature is 1305° F, and

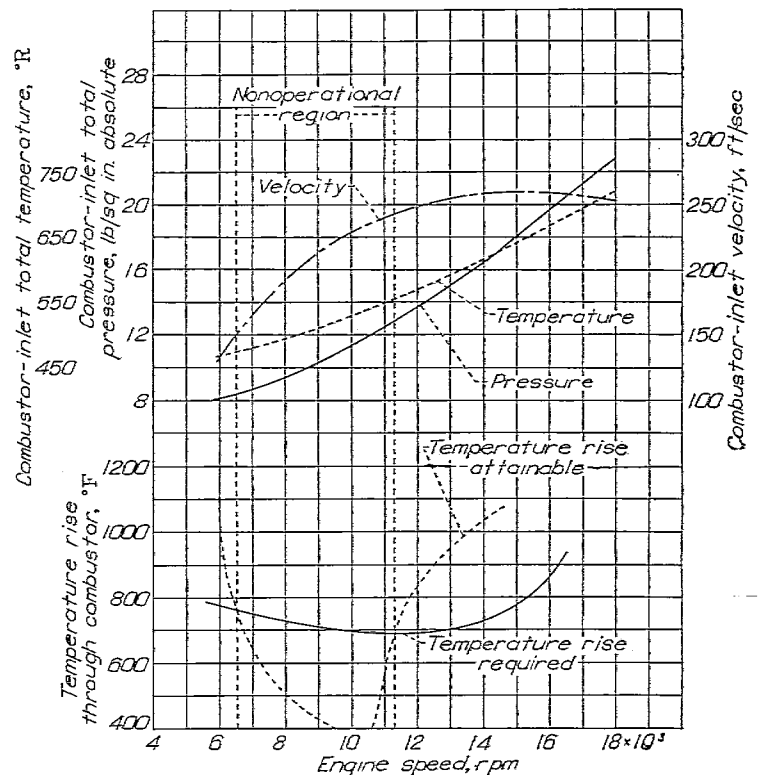


FIGURE 11.—Combustor operating conditions in jet-propulsion engine at various engine speeds at altitude of 20,000 feet. Static operation; tail cone retracted.

the average temperature-rise deviation from the mean temperature rise through the combustor is $\pm 111^\circ \text{F}$ (± 12.4 percent). In figure 13 (b) the mean outlet temperature is 1042°F , the minimum recorded local temperature is 640°F , the maximum recorded local temperature is 1600°F , and the average temperature-rise deviation from the mean temperature rise through the combustor is $\pm 156^\circ \text{F}$ (± 16.0 percent). The temperature profile is more uniform and the combustion efficiency is higher for the run presented in figure 13 (a) than for the run presented in figure 13 (b).

In check runs the outlet-temperature profiles could not always be exactly reproduced but consistent trends were indicated; the profiles became more uneven as the combustion efficiency became lower and as the temperature rise became higher. The localized high outlet temperatures (hot spots) became excessively high when the combustor basket was slightly off center. The positions of localized high temperatures also shifted from time to time, possibly as the result of progressive warping of the combustor basket.

The operating conditions listed in figures 13 (c) and 13 (d) simulated no particular altitude-engine-speed conditions but produced aggravated cases of uneven fuel distribution. The combustor-outlet temperature profiles are shown for these two runs in order to illustrate the effect of uneven fuel distribution. The causes of the uneven fuel distribution will be subsequently discussed.

In figure 13 (c) the mean outlet temperature is 240°F , the minimum recorded local temperature is 170°F , the maximum recorded local temperature is 310°F , and the average temperature-rise deviation from the mean temperature rise through the combustor is $\pm 31^\circ \text{F}$ (± 18.8 percent). The mean temperature rise for the bottom one-fourth of the duct is 35 percent higher than the mean temperature rise for the top one-fourth of the duct.

In figure 13 (d) the mean outlet temperature is 1222°F , the minimum recorded local temperature is 720°F , the maximum recorded local temperature is 1760°F , and the average temperature-rise deviation from the mean temperature rise through the combustor is $\pm 248^\circ \text{F}$ (± 28.1 percent). A low-temperature region occurs at the 1-o'clock position in the duct.

Typical velocity profiles at the combustor outlet are shown in figure 14 for three of the same runs for which temperature profiles appear in figure 13. The outlet-velocity profiles vary in uniformity as the outlet-temperature profiles vary; high local velocities usually result where high local temperatures occur. The velocities also definitely tended to remain low nearer the walls of the duct, regardless of temperature distribution. The inlet-velocity profiles are also shown in the figure for comparison.

EXTENT OF AFTERBURNING

The temperatures read at cross section 4 checked closely with those at cross section 3; no temperature rise due to

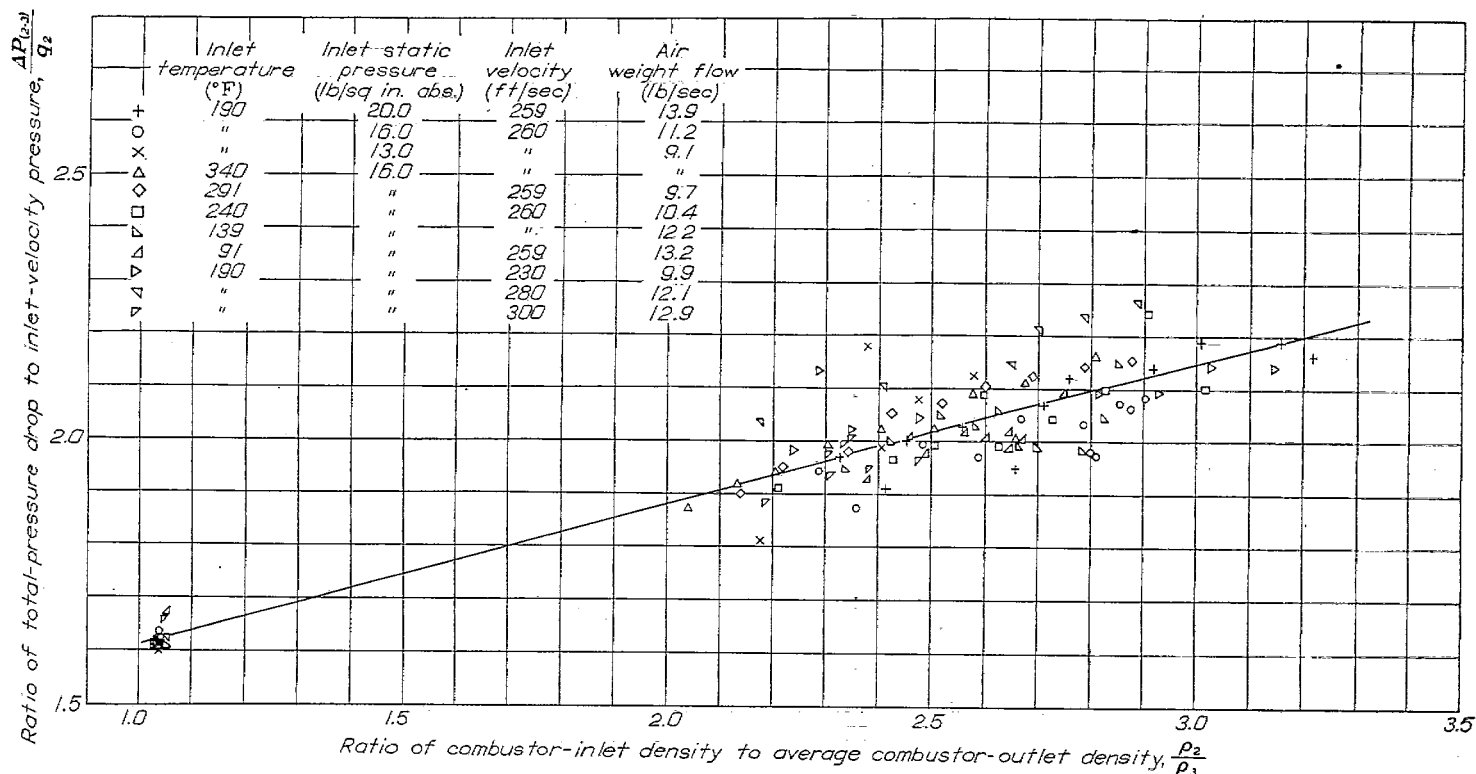
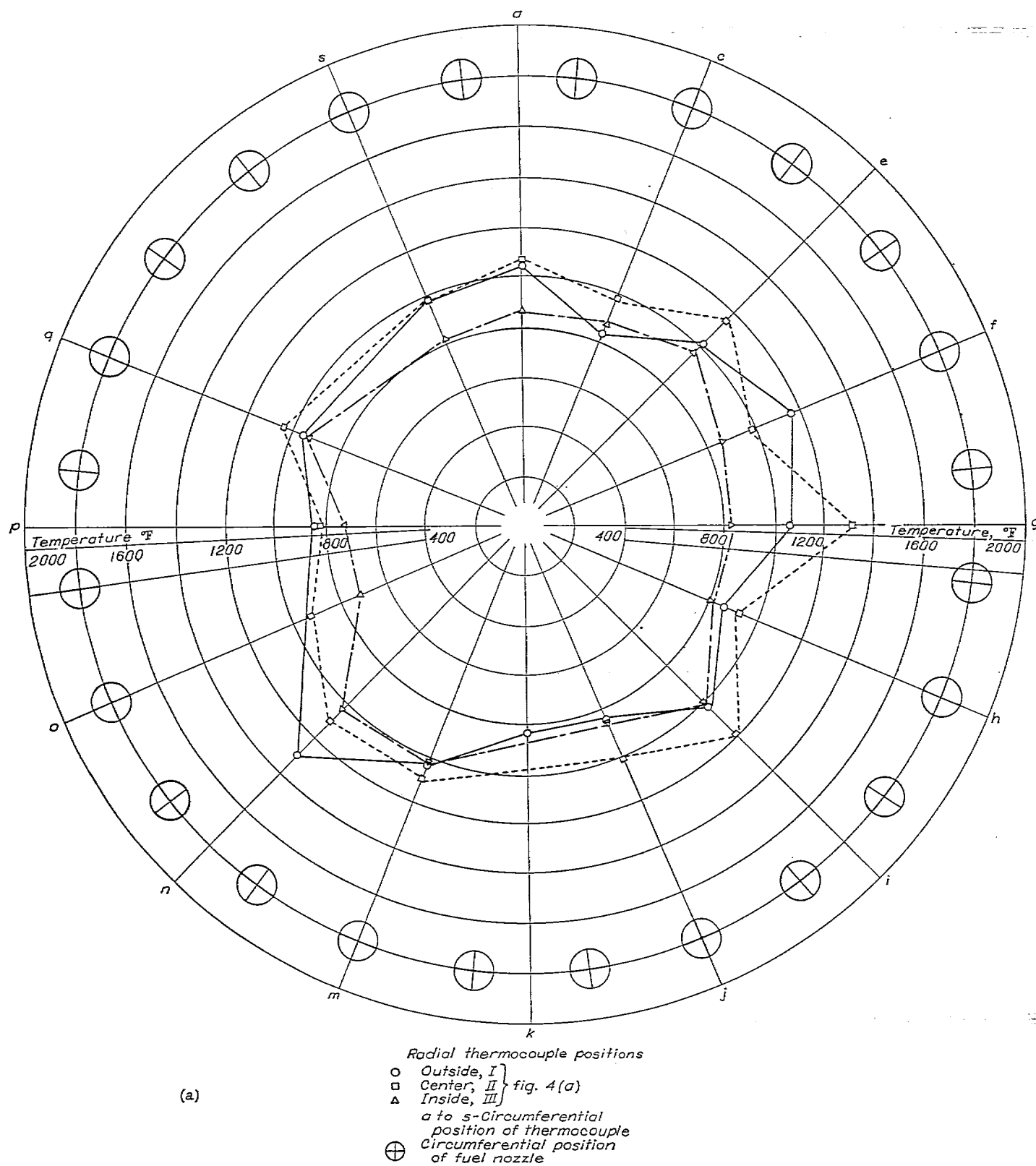
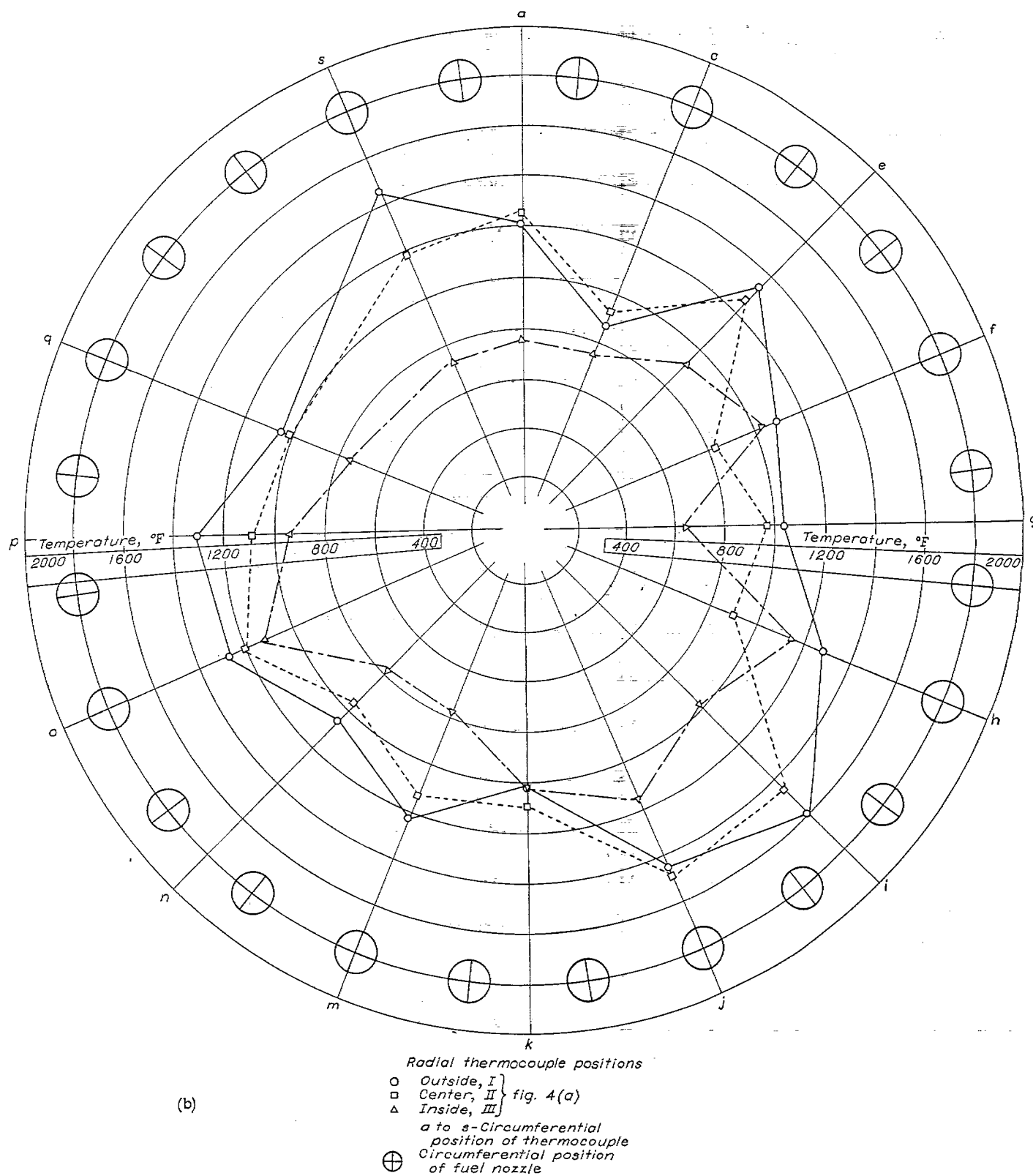


FIGURE 12.—Correlation of total-pressure drop through combustor. Data from study of effect of independently altering combustor-inlet parameters from values simulating static operation of engine at 15,500 rpm and altitude of 24,000 feet.



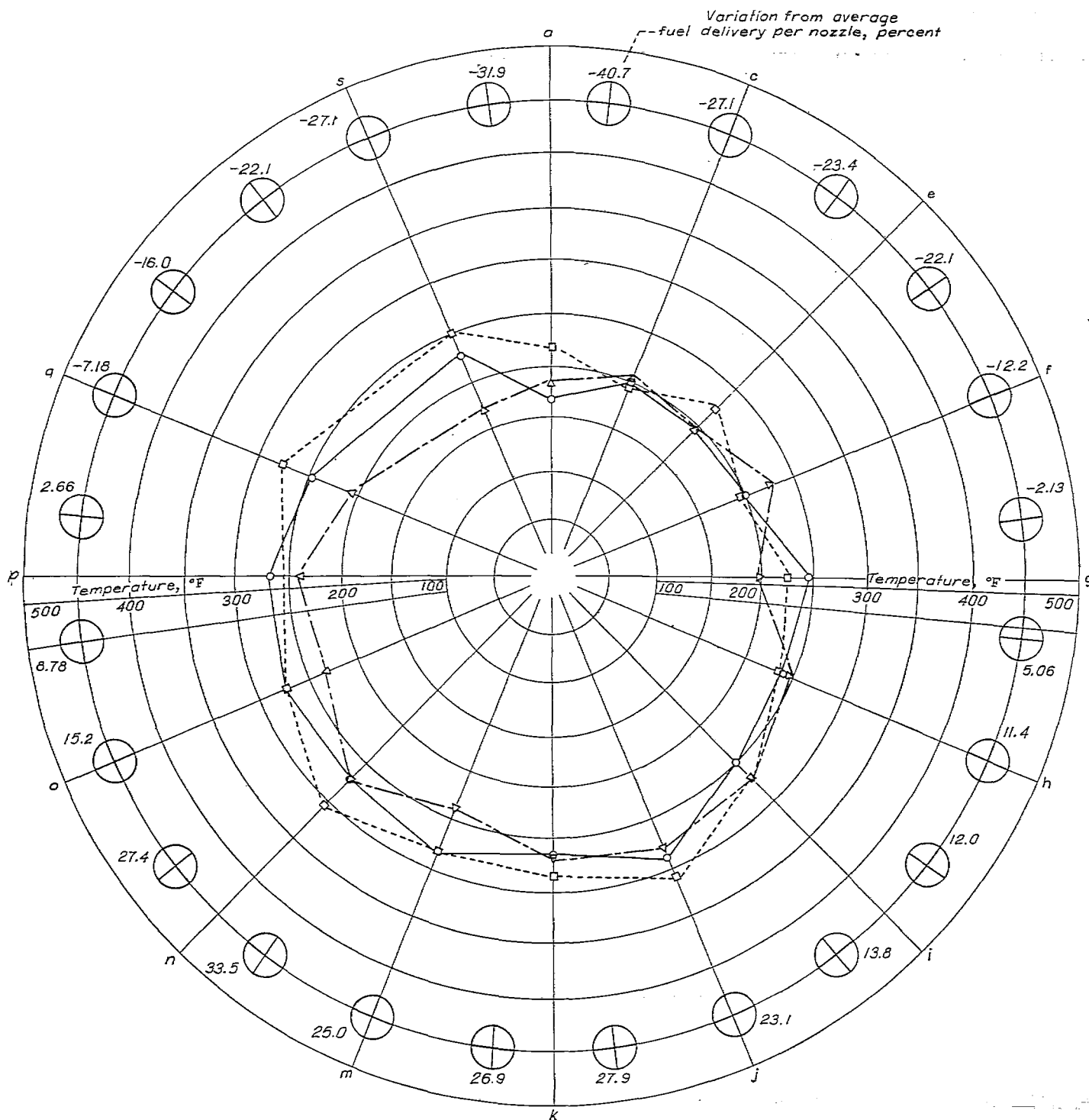
(a) Inlet static pressure, 13.41 pounds per square inch absolute; inlet temperature, 71° F; inlet velocity, 216 feet per second; fuel-air ratio, 0.0139; mean outlet temperature, 968° F.

FIGURE 13.—Temperature distribution at combustor outlet for representative runs.



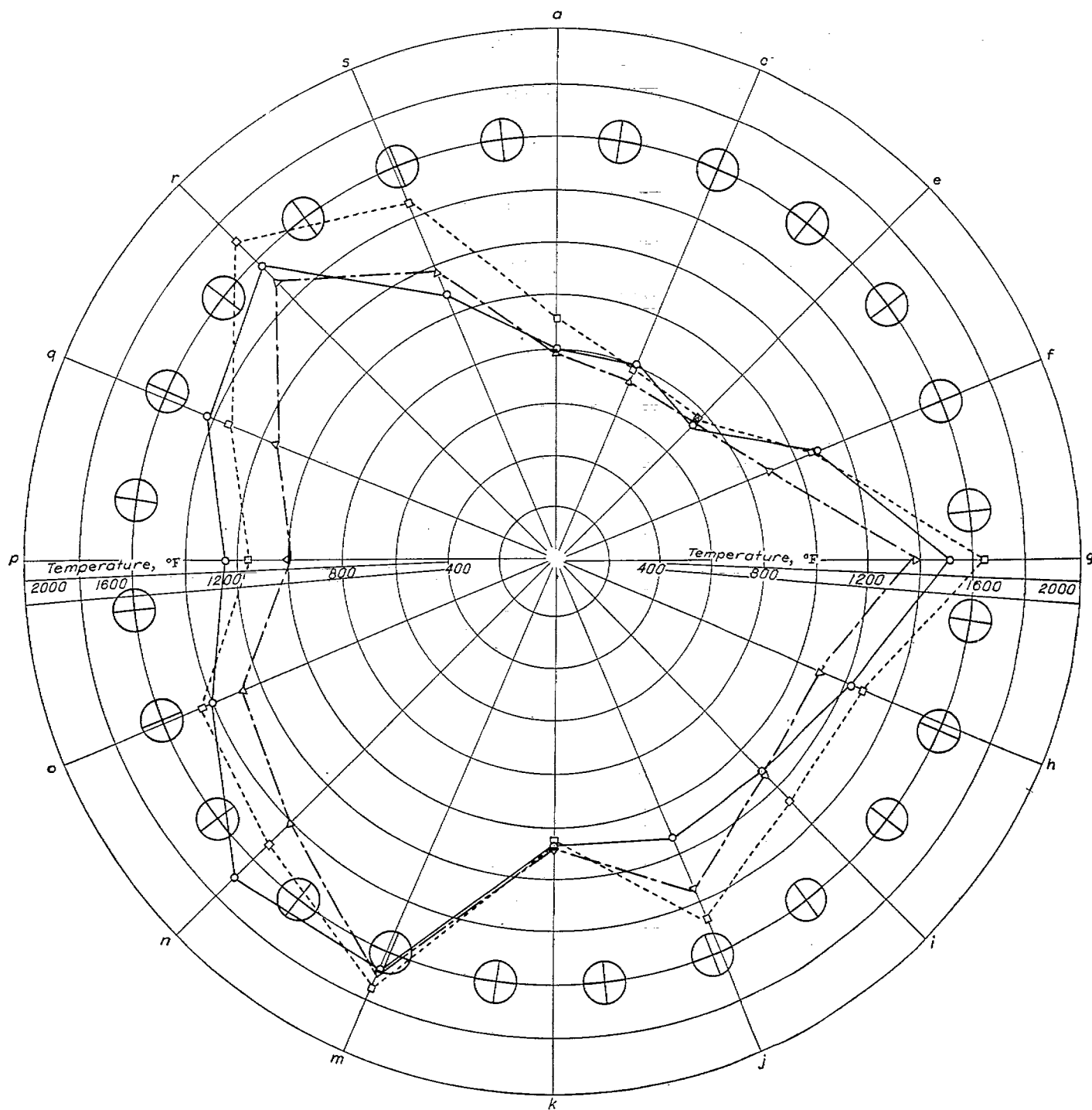
(b) Inlet static pressure, 13.39 pounds per square inch absolute; inlet temperature, 65° F; inlet velocity, 214 feet per second; fuel-air ratio, 0.016; mean outlet temperature, 1042° F.

FIGURE 13.—Continued.



(c) Inlet static pressure, 13.40 pounds per square inch absolute; inlet temperature, 75° F; inlet velocity, 197 feet per second; fuel-air ratio, 0.00322; mean outlet temperature, 240° F.

FIGURE 13.—Continued.



(d)

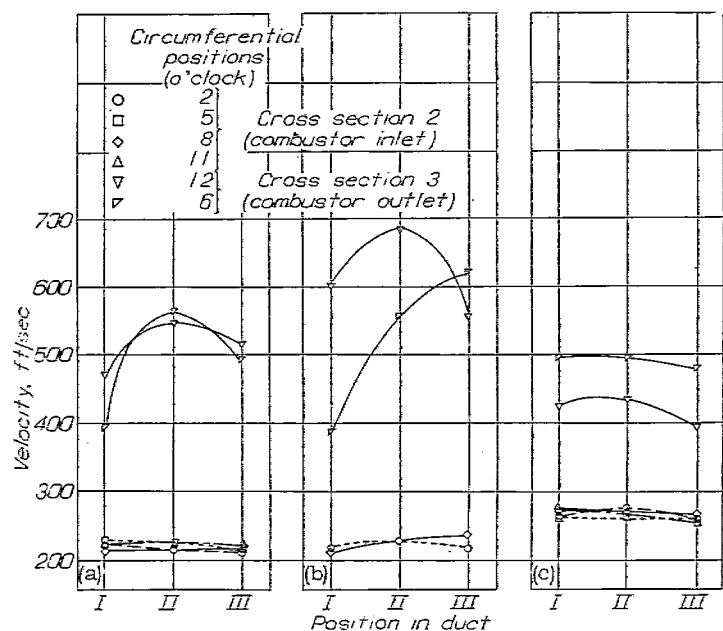
Radial thermocouple positions

- Outside, I
- Center, II
- △ Inside, III

a to s—Circumferential
position of thermocouple
⊕ Circumferential position
of fuel nozzle

(d) Inlet static pressure, 16.00 pounds per square inch absolute; inlet temperature, 340° F; inlet velocity, 260 feet per second; fuel-air ratio, 0.0130; mean outlet temperature, 1222° F.

FIGURE 13.—Concluded.



(a) Run shown in figure 13 (a).
 (b) Run shown in figure 13 (b).
 (c) Run shown in figure 13 (d).

FIGURE 14.—Velocity distribution at inlet and outlet of combustor for representative runs.

afterburning was therefore indicated in any of the tests. A tenuous luminous flame, however, appeared to extend past cross section 3 in some of the runs.

A comparison of the mean combustor-outlet temperatures at cross section 3 with temperatures read with a shielded thermocouple at the downstream cross section 5 is shown in figure 15. The downstream temperatures are lower than the mean values at the combustor outlet and the differences are greater at high temperatures. The calculated temperature drop in the exhaust gas, with allowance for heat transfer through the pipe walls between cross sections 3 and 5, was 40°F , with the exhaust-gas temperature assumed to be 1000°F at cross section 3 and the temperature of the test cell assumed to be 80°F . When the mean temperature at cross section 3 is 1000°F , figure 15 shows the measured temperature at cross section 5 to be about 40°F lower. The data points on figure 15 therefore deviate from the 45° line by the expected amount and the readings of the shielded thermocouple at cross section 5 check those of the bare-wire thermocouples at cross section 3.

CHARACTERISTICS OF FUEL-INJECTION SYSTEM

Hydraulic head in manifold.—The effect of the hydraulic head between the bottom and the top of the fuel manifold was evidenced during the investigation. As the fuel flow was decreased to a point where the pressure differential

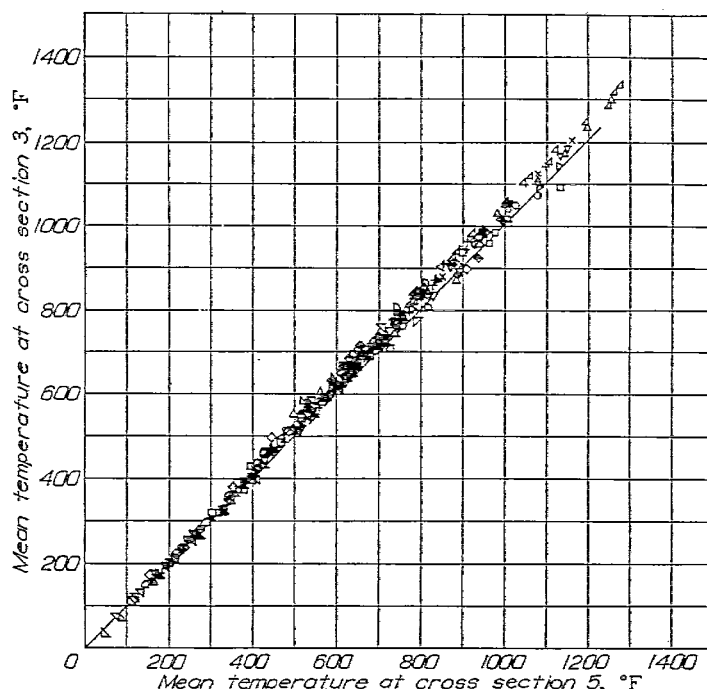


FIGURE 15.—Comparison of mean temperature at cross section 3 with mean temperature at cross section 5.

between the bottom of the manifold and the inside of the combustor approached the magnitude of the hydraulic head between the bottom and the top of the manifold, the nozzles at the top ceased to deliver enough fuel to sustain burning in that region. This partial cessation of burning always occurred at a fuel flow of about 75 pounds per hour.

The combustor-outlet temperature profile for a run in which the fuel flow was only 100 pounds per hour is shown in figure 13 (c). The fuel distribution and the outlet temperatures are higher at the bottom because of the hydraulic head within the manifold. The fuel nozzles were later calibrated while installed in the manifold by using a total fuel flow of about 100 pounds per hour; the results of this calibration are also shown in figure 13 (c). The percentage variation of each nozzle from the mean fuel delivery is given with each nozzle position.

Fuel deaeration and vaporization within fuel-injection system.—During the runs in which the inlet temperatures were 240°F and higher, dark areas were observed near the top of the ring of flame (looking upstream) even though the fuel flows were high enough to overcome the effect of the hydraulic head within the fuel manifold. These dark areas indicated the presence of air or vaporized fuel in the nozzles at the top of the manifold, where gases generated therein would collect. This condition will hereinafter be referred to as "vapor lock." A fuel nozzle, when delivering gases, loses some of the cooling effects of the fuel and becomes

overheated by the radiant heat from the flame, which aggravates the vapor-lock condition. It is reasonable to expect that under extreme conditions a vapor-locked nozzle could be heated to the extent that cracking of the fuel would cause the orifice to become clogged with carbonaceous deposits. During the investigation such carbonaceous deposits were formed in two nozzles.

This vapor-lock condition was investigated by peening iron-constantan thermocouples into the wall of the dome of each of three fuel nozzles in the manner previously described. Table III shows the nozzle temperatures observed during various runs. When the inlet temperatures exceeded 290° F, the fuel nozzle located near the top of the manifold (22.5° position) showed a sudden marked increase in temperature, which may be explained by a reduction in the mass flow of fuel through the nozzle due to the presence of vapors. The nozzles located lower in the manifold did not show this rapid change in temperature at any of the inlet temperatures investigated. Temperatures within and above the boiling range of the fuel were attained in all three nozzles, indicating that vaporization of the fuel as well as deaeration was causing this trouble.

One manifestation of vapor lock is shown in figure 16 where the pressure differential across the fuel manifold and nozzles is plotted against the fuel flow for runs made with the same set of fuel nozzles. The pressure differential for a given fuel flow is seen to increase with combustor-inlet temperature after a critical inlet temperature is surpassed. As the fuel flow increases, the vapor-lock effect becomes less, as shown by the converging curves in figure 16.

Figure 13 (d) shows the combustor-outlet temperature profile for a run in which the inlet temperature was 340° F; deaeration and vaporization of the fuel within the fuel-injection system had resulted in vapor lock of the fuel nozzles at the top of the manifold and extinguished the flame at the 12- and 1-o'clock positions.

CONDITION OF COMBUSTOR BASKET

Warping of the combustor basket existed in places where local temperatures were high but the distortion never became excessive. No holes were burned in the basket during the tests, and no carbonaceous deposits thicker than 0.002 inch were found on the walls of the basket. At the altitude conditions of most of the tests reported herein, blue-flame combustion prevailed; at low altitude where yellow-flame combustion occurred, warping and the formation of carbonaceous deposits became greater than with blue flames.

SUMMARY OF RESULTS

A combustion-laboratory investigation of the performance of an annular combustor gave the following results:

1. The lowest operational ceiling of the complete engine

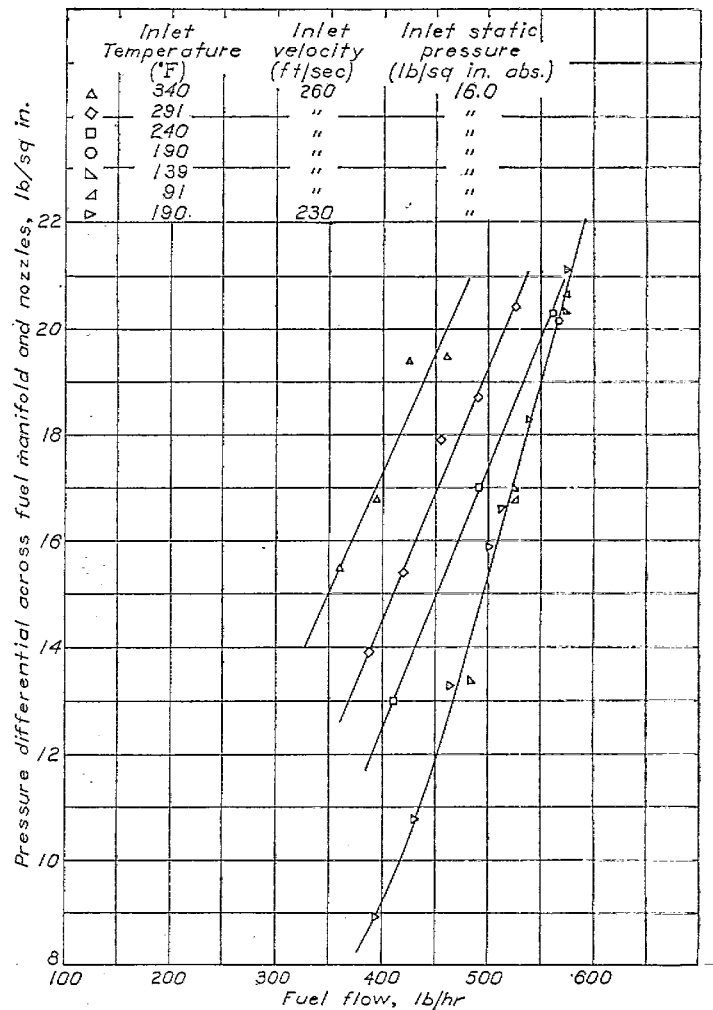


FIGURE 16.—Pressure differential measured across fuel manifold and nozzles as function of fuel flow for all runs with same set of fuel nozzles.

as determined by tests of the combustor operating with AN-F-22 fuel was at an altitude of 16,400 feet and occurred at a simulated engine speed of 8000 rpm. At a simulated engine speed of 17,500 rpm, the combustor operated satisfactorily to an altitude of 34,000 feet.

2. With AN-F-28 fuel, the minimum operational ceiling was at 14,600 feet and also occurred at a simulated engine speed of 8000 rpm. At simulated engine speeds close to the rated maximum of 18,000 rpm, operation was satisfactory to altitudes higher than 30,000 feet.

3. At altitudes of 8000 feet or more below the operational limits, the combustor operated at efficiencies higher than 90 percent and was capable of producing outlet temperatures far in excess of the engine requirements.

4. As the simulated altitude was progressively increased, approaching the operational limits: (1) Resonant combustion began and became increasingly severe; (2) the combustion efficiency decreased; and (3) the temperature rise through the combustor began to pass through a maximum value

(with increase in fuel-air ratio) at a fuel-air ratio within the range investigated. Both the maximum temperature rise obtainable and fuel-air ratio at which it occurred decreased as the simulated altitude was increased. Above the operational limits, the maximum obtainable temperature rise was below the value required for engine operation.

5. High combustor-inlet pressures and temperatures and low combustor-inlet velocities were favorable to combustion. When these combustor-inlet conditions were favorable to combustion, the combustor operated at efficiencies above 95 percent and the temperature rise through the combustor increased with an increase in fuel-air ratio throughout the range of fuel-air ratios investigated.

6. The combustion efficiency and maximum temperature rise obtainable decreased and resonance increased if: (1) The combustor-inlet pressure was decreased, (2) the combustor-inlet temperature was decreased, or (3) the combustor-inlet velocity was increased. Both the maximum obtainable combustor temperature rise and fuel-air ratio at which it occurred decreased as these inlet conditions became more adverse.

7. The existence of altitude operational limits was accounted for by the effects of the combustor-inlet conditions on combustor performance.

8. The ratio of the total-pressure drop through the com-

burntor to the inlet velocity pressure correlated as a linear function of the ratio of the combustor-inlet density to the combustor-outlet density. The linear relation was predicted by theoretical considerations. The isothermal total-pressure drop through the combustor was 1.62 times as great as the inlet velocity pressure.

9. Combustor-outlet temperature profiles became increasingly uneven as the temperature rise increased or as the combustion efficiency decreased.

10. Thermocouples located downstream of the combustor indicated temperatures consistent with those measured at the combustor outlet; no temperature rise due to afterburning was detected.

11. Vaporization and deaeration of fuel within the fuel manifold and nozzles led to severe overheating of the nozzles, which caused nonuniform combustor-outlet temperature distributions and sometimes resulted in the formation of carbonaceous deposits in the fuel nozzles.

12. Very little deterioration of the combustor basket occurred and no carbonaceous deposits thicker than 0.002 inch were present.

FLIGHT PROPULSION RESEARCH LABORATORY,
NATIONAL ADVISORY COMMITTEE FOR AERONAUTICS,
CLEVELAND, OHIO, *March 21, 1947.*

APPENDIX

ANALYSIS OF TOTAL-PRESSURE DROP THROUGH COMBUSTOR

The following symbols are used in the analysis:

- A cross-sectional area of combustion space, sq ft
- k_1, k_2 dimensionless constants
- m mass flow per unit cross-sectional area, slugs/(sec) (sq ft)
- q dynamic pressure, lb/sq ft
- ΔP total-pressure drop, lb/sq ft
- Δp static-pressure drop, lb/sq ft
- V velocity, ft/sec
- ρ density, slugs/cu ft
- Subscripts (See fig. 1.):
- 2 combustor inlet
- 3 combustor outlet
- f friction
- m momentum

The total-pressure drop due to friction can be expressed as

$$(\Delta P_{2-3})_f = k_1 \frac{\rho_2 V_2^2}{2} \quad (1)$$

When a simplified combustor of constant cross section is assumed, the static-pressure drop due to momentum change is

$$(\Delta p_{2-3})_m = \frac{m}{A} (V_3 - V_2) \quad (2)$$

and the total-pressure drop due to momentum change is

$$(\Delta P_{2-3})_m = \frac{m}{A} (V_3 - V_2) + \frac{\rho_2 V_2^2}{2} - \frac{\rho_3 V_3^2}{2} \quad (3)$$

The total-pressure drop through the combustor is the sum

of the pressure drop due to friction and the pressure drop due to momentum change:

$$\Delta P_{2-3} = k_1 \frac{\rho_2 V_2^2}{2} + \frac{m}{A} (V_3 - V_2) + \frac{\rho_2 V_2^2}{2} - \frac{\rho_3 V_3^2}{2} \quad (4)$$

Substitution of $\rho_2 A V_2$ for m gives

$$\Delta P_{2-3} = k_1 \frac{\rho_2 V_2^2}{2} + \rho_2 V_2^2 \left(\frac{V_3}{V_2} - 1 \right) + \frac{\rho_2 V_2^2}{2} \left(1 - \frac{\rho_3 V_3^2}{\rho_2 V_2^2} \right) \quad (5)$$

When the slight increase in mass due to the addition of fuel between the combustor inlet and the combustor outlet is neglected,

$$\rho_2 V_2 = \rho_3 V_3 \quad (6)$$

or,

$$\frac{V_3}{V_2} = \frac{\rho_2}{\rho_3} \quad (7)$$

If equation (7) is substituted in equation (5) and the terms are combined,

$$\Delta P_{2-3} = \frac{\rho_2 V_2^2}{2} \left(\frac{\rho_2}{\rho_3} + k_1 - 1 \right) \quad (8)$$

Substitution of q_2 for $\frac{\rho_2 V_2^2}{2}$ and k_2 for $(k_1 - 1)$ gives

$$\frac{\Delta P_{2-3}}{q_2} = \frac{\rho_2}{\rho_3} + k_2 \quad (9)$$

For any particular combustor, equation (9) is valid only if q_2 is equal to, or has a fixed ratio to, the effective value of q .

TABLE I—PERFORMANCE DATA ON COMBUSTOR FROM INVESTIGATION TO DETERMINE ALTITUDE OPERATIONAL LIMITS WITH AN-F-22 FUEL

Point	Simulated engine speed (rpm)	Simulated altitude (ft)	Combustor-inlet static pressure (lb/sq in. absolute)	Combustor-inlet temperature (° F)	Combustor-inlet velocity (ft/sec)	Air flow (lb/sec)	Fuel flow (lb/hr)	Fuel-air ratio	Mean combustor-outlet temperature (° F)	Mean temperature rise through combustor (° F)	Ratio of actual to theoretical temperature rise	Total-pressure drop through combustor (lb/sq in.)	Static-pressure drop through combustor (lb/sq in.)	Type of resonance (1)
1	10,000	16,600	13.19 13.19 13.19	84 84 84	226 226 226	9.58 9.58 9.58	600 632 654	0.0174 .0153 .0190	1,006 1,160 931	1,012 1,076 847	0.818 .832 .633	0.82 .83 .79	1.13 1.16 1.02	B- B- D
2	10,000	20,000	11.10 11.10	74 74	233 233	8.51 8.50	377 405	0.0123 .0132	----- -----	Outlet temperatures below 400° F Blow-out				A A
3	10,000	23,000	9.48 9.48	64 64	240 240	7.59 7.59	395 405	0.0145 .0148	----- -----	Outlet temperatures below 400° F Blow-out				A A
4	10,000	30,000	6.40	45	271	6.00	-----	-----	-----	No combustion				
5	15,000	30,000	11.32 11.32	177 177	277 277	8.62 8.62	422 440	0.0136 .0142	600 -----	423	0.434 Blow-out	0.76 -----	0.78 -----	E- A+
6	16,000	30,000	12.50 12.48 12.48	207 207 207	264 264 264	8.69 8.69 8.69	575 595 750	0.0184 .0190 .0240	1,230 983 -----	1,023 776	0.796 .587 Blow-out	0.85 .78 -----	1.10 .93 -----	B- D+ D+
7	17,000	30,000	13.51	240	255	8.61	705	0.0227	1,474	1,234	0.801	0.80	1.09	D-
8	18,000	30,000	14.69 14.69	274 275	233 233	8.18 8.19	595 652	0.0202 .0221	1,569 1,654	1,295 1,379	0.938 .917	0.72 .75	0.96 1.01	B B-
9	16,500	40,000	9.80 9.80	140 140	241 241	6.89 6.89	403 445	0.0162 .0179	621 -----	481	0.418 Blow-out	0.55 -----	0.58 -----	A A+

¹The various types of resonant combustion are designated as follows: A, rapid flickering at base of flame; B, temperature fluctuations at combustor outlet; C, noisy vibration of combustor and adjacent ducting; D, combination of B and C; E, combination of A and B; N, normal operation (no noticeable resonance); +, severe; -, slight.

TABLE I—PERFORMANCE DATA ON COMBUSTOR FROM INVESTIGATION TO DETERMINE ALTITUDE OPERATIONAL LIMITS WITH AN-F-22 FUEL—Concluded

Point	Simulated engine speed (rpm)	Simulated altitude (ft)	Combustor-inlet static pressure (lb/sq in. absolute)	Combustor-inlet temperature (° F)	Combustor-inlet velocity (ft/sec)	Air flow (lb/sec)	Fuel flow (lb/hr)	Fuel-air ratio	Mean combustor-outlet temperature (° F)	Mean temperature rise through combustor (° F)	Ratio of actual to theoretical temperature rise	Total pressure drop through combustor (lb/sq in.)	Static pressure drop through combustor (lb/sq in.)	Type of resonance (1)
10	16,000	32,000	11.19 11.19 11.19 11.19	205 206 206 205	270 270 270 270	7.97 7.97 7.97 7.97	363 385 420 450	0.0123 .0134 .0146 .0176	781 827 704	576 621 499	0.631 .646 .490	0.74 .76 .73	0.89 .83 .76	N B- A A
11	16,500	30,000	12.88 12.88 12.88	224 225 225	266 267 267	8.78 8.80 8.79	570 610 630	0.0180 .0193 .0199	1,282 1,362 1,015	1,038 1,137 790	0.842 .850 .574	0.89 .90 .85	1.14 1.18 1.00	N N E-
12	15,500	30,000	11.98 11.95 11.98 12.42	193 192 192 192	267 266 266 256	8.58 8.56 8.56 8.56	470 500 630 800	0.0152 .0162 .0204 .0260	990 799 851	797 607 659	0.741 .831 .467	0.83 .80 .78	0.99 .89 .89	A- E E+ A+
13	14,000	20,000	16.39	162	264	12.19	785	0.0179	1,298	1,136	0.905	1.16	1.61	B-
14	14,000	24,000	13.71 13.71 13.68	155 155 155	270 272 272	10.58 10.61 10.61	582 596 608	0.0153 .0156 .0159	988 1,003 774	833 848 619	0.766 .765 .549	1.01 1.02 1.00	1.25 1.28 1.14	B B E
15	14,000	30,000	10.15 10.19	150 150	254 254	8.30 8.25	395 456	0.0132 .0154	-----	Outlet temperatures below 400° F Blow-out				A A
16	14,500	28,000	11.88 11.88 11.88 11.88	162 161 162 162	272 275 275 275	9.15 9.20 9.20 9.20	460 420 550 600	0.0140 .0157 .0166 .0181	619	458	0.458	0.83	0.87	A+ A+ A+ A+
17	12,000	17,000	15.07 15.07 15.00	127 126 126	256 256 258	11.60 11.60 11.61	760 770 795	0.0182 .0184 .0190	1,234 1,203 922	1,109 1,078 797	0.865 .832 .599	1.05 1.09 1.06	1.49 1.52 1.33	C- D- D+
18	12,000	19,000	14.18 14.18 14.18	120 120 120	256 256 256	11.03 11.01 11.01	688 730 900	0.0173 .0184 .0227	1,122 882	1,002 762	0.817 .558	1.02 .97	1.39 1.20	N E A+
19	12,000	30,000	8.19 8.22 8.22	88 91 91	263 263 263	7.40 7.40 7.40	355 550 600	0.0133 .0206 .0225	-----	Outlet temperatures below 400° F Outlet temperatures below 400° F Blow-out				A A A+
20	15,500	28,000	13.10 13.10 13.10	191 191 191	264 264 264	9.30 9.30 9.30	605 640 900	0.0181 .0191 .0269	1,231 981 940	1,040 790 749	0.821 .596 .418	0.92 .86 .83	1.20 1.03 .99	N E E+
21	8,000	17,000	10.41 10.41 10.41	50 50 50	198 198 198	7.09 7.09 7.09	305 350 390	0.0120 .0137 .0153	-----	Outlet temperatures below 400° F Blow-out				A A A+
22	8,000	19,000	9.78 9.78 9.78	44 45 45	198 198 198	6.71 6.70 6.70	315 346 385	0.0130 .0143 .0160	-----	Outlet temperatures below 400° F Outlet temperatures below 400° F Blow-out				A A+ A+
23	14,000	26,000	12.39 12.39 12.39	153 153 153	277 277 277	9.78 9.78 9.78	375 393 500	0.0107 .0112 .0142	599 539	446 356	0.570 .472	0.88 .85	0.92 .86	B- E- A
24	13,000	23,000	13.10 13.10 13.10	133 132 132	263 263 263	10.19 10.19 10.19	500 538 730	0.0136 .0147 .0199	881 694	748 562	0.763 .531	0.92 .89	1.12 1.00	N A A+
25	6,000	20,000	7.99 7.99 7.99 7.99	17 17 17 17	142 142 142 142	4.17 4.17 4.17 4.17	332 350 373 400	0.0221 .0233 .0248 .0266	1,197	1,180	0.761	0.24	0.36	D- A A A+
26	6,000	24,000	6.40	8	137	3.30	-----	-----	-----	No combustion				
27	12,000	21,000	12.98 12.98 12.98	113 113 112	255 255 255	10.14 10.14 10.14	475 500 590	0.0130 .0137 .0162	812 636	609 523	0.742 .528	0.88 .85	1.06 .94	N A A+
28	10,000	18,500	11.89 11.89 11.89	79 80 80	230 230 230	8.88 8.88 8.88	400 435 466	0.0125 .0136 .0152	711 591	632 511	0.693 .513	0.70 .67	0.82 .74	B- E A+
29	8,000	21,000	8.70 8.70	40 40	199 199	6.20 6.20	335 350	0.0153 .0160	-----	Outlet temperatures below 400° F Blow-out				A A+
30	6,000	16,000	9.87 9.87 9.87	22 21 22	144 144 144	5.17 5.17 5.17	396 525 590	0.0213 .0252 .0317	1,171 1,374	1,149 1,353	0.767 .707	0.38 .42	0.52 .60	N A- A+
31	17,500	32,000	13.31	265	261	8.41	570	0.0188	1,447	1,182	0.912	0.84	1.09	B
32	19,000	30,000	16.80	310	207	7.92	500	0.0175	1,490	1,180	0.974	0.60	0.76	N
33	12,000	24,000	11.40 11.40	103 103	261 261	9.29 9.29	380 415	0.0114 .0124	-----	353	0.423	-----	-----	E A
34	17,500	34,000	11.89	261	241	6.98	450	0.0179	1,378	1,117	0.899	0.63	0.80	B-
35	8,000	15,500	11.21 11.23 11.21	56 58 58	196 198 198	7.49 7.50 7.50	410 429 510	0.0152 .0159 .0189	927 971	871 913	0.794 .800	0.53 .55	0.70 .73	B- B- A+
36	17,500	36,000	10.19 10.19 10.17	260 260 260	261 261 263	6.50 6.50 6.50	316 350 400	0.0135 .0150 .0171	938 837	678 577	0.708 .546	0.53 .54	0.59 .57	B E A

TABLE II—PERFORMANCE DATA ON COMBUSTOR FROM INVESTIGATION TO DETERMINE ALTITUDE OPERATIONAL LIMITS WITH AN-F-28, AMENDMENT-3, FUEL

Point	Simulated engine speed (rpm)	Simulated altitude (ft)	Combustor-inlet static pressure (lb/sq in. absolute)	Combustor-inlet temperature (° F)	Combustor-inlet velocity (ft/sec)	Air flow (lb/sec)	Fuel flow (lb/hr)	Fuel-air ratio	Mean combustor-outlet temperature (° F)	Mean temperature rise through combustor (° F)	Ratio of actual to theoretical temperature rise	Total pressure drop through combustor (lb/sq in.)	Static pressure drop through combustor (lb/sq in.)	Type of resonance (1)
1	10,000	16,000	13.20 13.20 13.20	88 88 88	229 229 229	9.63 9.63 9.63	425 450 480	0.0123 .0130 .0138	755 780 -----	668 692 -----	Blow-out 0.751 .740 0.80 .84		0.94 .97	N B- A+
3	10,000	23,000	9.50 9.50	65 65	240 240	7.58 7.58	320 370	0.0117 .0136	-----	Outlet temperature below 400° F Blow-out				A+ A+
8	18,000	30,000	14.70 14.70	274 274	233 233	8.19 8.19	670 900	0.0193 .0204	1510 1541	1236 1267	0.945 .921	0.73 .74	0.96 .99	N N
10	16,000	32,000	11.20 11.20 11.20	205 203 205	269 267 269	7.95 7.93 7.95	300 358 400	0.0103 .0120 .014	632 624 -----	427 421 -----	0.562 .460 Blow-out	0.68 .67	0.69 .67	E- A+ A+
11	16,500	30,000	12.90 12.90 12.90	224 223 225	266 266 266	8.79 8.79 8.79	401 472 500	0.0127 .0149 .0168	916 1028 -----	692 805 -----	0.767 .772 Blow-out	0.78 .82	0.88 .96	A- N A+
13	14,000	20,000	16.39 16.40	162 162	264 264	12.20 12.20	640 770	0.0146 .0175	1042 -----	880 -----	0.866 Blow-out	1.15	1.45	N A+
14	14,000	24,000	13.38 13.71	154 155	272 270	10.61 10.60	450 480	0.0118 .0126	573 -----	419 -----	0.494 Blow-out	0.89	0.92	A+ A+
17	12,000	17,000	15.09 15.09	125 124	256 256	11.63 11.63	503 600	0.0120 .0143	829 949	704 825	0.812 .811	1.02 1.05	1.22 1.32	N N
18	12,000	19,000	14.18 14.18 14.18	120 120 120	256 256 256	11.00 11.00 11.00	413 442 465	0.0104 .0112 .0117	675 710 -----	555 590 -----	0.730 .725 Blow-out	0.95 .97	1.06 1.10	N A- A+
20	15,500	28,000	13.12 13.09	181 191	263 263	9.29 9.29	460 490	0.0138 .0147	916 -----	725 -----	0.744 Blow-out	0.82	0.95	A- A+
21	8,000	17,000	10.41 10.41	50 50	198 199	7.08 7.15	355 406	0.0139 .0158	537 -----	487 -----	0.488 Blow-out	0.45	0.49	A- A+
23	14,000	26,000	12.38 12.38 12.38	155 155 152	275 275 277	9.74 9.74 9.74	380 405 440	0.0108 .0116 .0125	520 -----	368 -----	Outlet temperatures below 400° F Blow-out		0.81 0.81	A- A+ A+
25	6,000	20,000	7.99 7.99 7.99	11 11 11	141 141 141	4.20 4.20 4.20	255 295 350	0.0169 .0195 .0231	654 761 -----	643 740	0.535 .541 Blow-out	0.27 .30	0.32 .36	E+ E+ -----
30	6,000	16,000	9.88 9.88 9.88	23 22 22	145 145 145	5.20 5.20 5.20	360 470 550	0.0192 .0251 .0294	1055 1293 -----	1032 1271	0.766 .746 Blow-out	0.35 .39	0.47 .55	E- E- -----
31	17,500	32,000	13.32 13.32	264 265	260 261	8.40 8.40	515 605	0.0170 .0200	1288 1424	1024 1169	0.877 .865	0.78 .80	0.87 1.05	N N
33	12,000	24,000	11.40 11.40 11.40	103 103 103	261 263 261	9.30 9.31 9.30	365 386 423	0.0109 .0115 .0126	----- ----- -----	Outlet temperature below 400° F Outlet temperature below 400° F Blow-out				A- A+ A+
34	17,500	34,000	11.90 11.90	260 260	241 241	7.30 7.00	448 498	0.0178 .0198	1541 1457	1081 1197	0.889 .893	0.61 .63	0.77 .83	N N
35	8,000	15,600	11.19 11.19 11.19	58 58 58	198 198 198	7.50 7.49 7.50	360 410 415	0.0133 .0152 .0154	554 -----	496 -----	0.518 Blow-out Blow-out	0.50	0.55	A+ A+ A+
37	16,000	25,000	15.80 15.80	203 202	258 258	10.77 10.77	605 658	0.0156 .0170	1198 1278	995 1076	0.915 .915	1.00 1.08	1.28 1.34	N E-
39	8,000	14,000	11.99 11.99	51 52	194 194	7.97 7.97	465 495	0.0162 .0173	826 -----	875 -----	0.732 Blow-out	0.63	0.81	E- -----
40	8,000	13,000	12.51 12.60	53 52	194 194	8.29 8.30	525 550	0.0176 .0184	1056 -----	1003 -----	0.810 Blow-out	0.39	0.92	E- A
42	17,000	28,000	15.10 15.11	240 240	246 246	9.31 9.32	550 675	0.0164 .0201	1297 1436	1057 1246	0.933 .914	0.84 -----	1.06 1.18	B- D-
43	16,500	34,000	10.70 10.70	225 225	269 269	7.30 7.30	345 400	0.0130 .0151	508 -----	383 -----	0.415 Blow-out	0.67	0.66	E E+
45	6,000	13,000	10.69 10.67 10.68	31 30 29	144 144 144	5.50 5.50 5.60	400 463 525	0.0202 .0234 .0265	1162 1281 1499	1131 1251 1470	0.802 .779 .824	0.39 .43 .41	0.53 .59 .62	A- E E

1 The various types of resonant combustion are designated as follows: A, rapid flickering at base of flame; B, temperature fluctuations at combustor outlet; C, noisy vibration of combustor and adjacent ducting; D, combination of B and C; E, combination of A and B; N, normal operation (no noticeable resonance); +, severe; -, slight.

TABLE III—TEMPERATURES OF THREE FUEL NOZZLES IN COMBUSTOR

Inlet static pressure (lb/sq in. absolute)	Inlet temperature (° F)	Inlet velocity (ft/sec)	Air flow (lb/sec)	Fuel flow (lb/hr)	Fuel-air ratio	Fuel-manifold pressure differential (lb/sq in.)	Temperature (° F)		
							Position of nozzle (arranged counterclockwise, looking upstream)		
							187.5°	97.5°	22.5°
10.67	72	217	7.64	446	0.0162	8.35	78	87	79
10.67	72	217	7.64	479	.0174	9.53	78	78	72
13.41	127	217	8.71	280	.0089	8.59	121	179	141
13.41	127	218	8.73	343	.0109	12.28	120	168	152
13.41	172	215	8.00	258	.0089	7.56	150	190	150
13.41	172	215	8.00	315	.0109	11.00	163	173	170
16.01	289	260	9.73	384	.0110	9.01	230	210	268
15.98	290	260	9.73	453	.0129	12.47	230	200	238
15.98	287	259	9.71	523	.0150	14.34	230	192	248
15.98	290	260	9.71	595	.0170	17.19	230	185	245
15.98	339	259	9.09	360	.0110	9.67	266	229	472
15.98	339	259	9.09	426	.0130	12.08	265	162	496
15.98	340	259	9.07	458	.0140	13.45	265	159	424
15.98	340	259	9.09	491	.0150	15.59	265	156	407

TSOIN FORM 69 (13 MAR 47)

Childs, J. H.
McCafferty, R. J.
Surine, O. W.

DIVISION: Power Plants, Jet and Turbine (5)
SECTION: Combustion Chambers (12)
CROSS REFERENCES: Combustion chambers - Testing (23865);
Combustion chambers - Turbo-jet
(23900)

ATI- 6594

ORIG. AGENCY NUMBER

TN-1357

REVISION

AUTHOR(S)

AMER. TITLE: Effect of combustor inlet conditions on performance of an annular turbojet combustor

FORG'N. TITLE:

ORIGINATING AGENCY: National Advisory Committee for Aeronautics, Washington, D. C.

TRANSLATION:

COUNTRY	LANGUAGE	FORG'N. CLASS	U. S. CLASS.	DATE	PAGES	ILLUS.	FEATURES
U.S.	Eng.		Unclass.	Jul '47	52	31	tables, diagrs, graphs

ABSTRACT

Combustion performance and altitude operational limits were studied over a wide range of air and fuel flows, inlet pressures, and temperatures. Combustion efficiencies, pressure losses, temperature, and velocity at combustion chamber outlet were determined. Extent of afterburning and fuel injection characteristics were observed. At altitudes of 8000 feet or more below operational limits, combustion chamber operated at efficiency of 90% and was capable of producing outlet temperatures far in excess of engine requirements.

NOTE: Requests for copies of this report must be addressed to: N.A.C.A.,
Washington, D. C.

T-2, HQ., AIR MATERIEL COMMAND

AIR TECHNICAL INDEX

WRIGHT FIELD, OHIO, USAAF

WF-O-21 MAR 47 2024